CHALMERS

NORDTEST

NORDTEST project No. 1672-04
Application of WST-method for fracture testing of fibre-reinforced cement based composites

BYG•DTU
DTU Department of Civil engineering

CHALMERS

Swedish National Testing and Research Institute

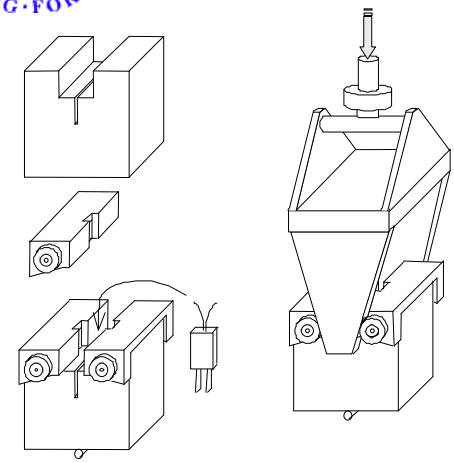

Application of WST-method for fracture testing of fibre-reinforced concrete

INGEMAR LÖFGREN, JOHN FORBES OLESEN AND MATHIAS FLANSBJER

Department of Structural Engineering and Mechanics
Concrete Structures
CHALMERS UNIVERSITY OF TECHNOLOGY
Göteborg, Sweden 2004

Report 04:13

REPORT 04:13

Application of WST-method for fracture testing of fibre-reinforced concrete

INGEMAR LÖFGREN, JOHN FORBES OLESEN
AND MATHIAS FLANSBJER

Department of Structural Engineering and Mechanics
Concrete Structures

CHALMERS UNIVERSITY OF TECHNOLOGY
Göteborg, Sweden 2004

Application of WST-method for fracture testing of fibre-reinforced concrete

INGEMAR LÖFGREN[I], JOHN FORBES OLESEN[II] AND MATHIAS FLANSBJER[III]

[I]Department of Structural Engineering and Mechanics, Chalmers University of Technology.

[II]DTU – Technical University of Denmark, Department of Civil Engineering.

[III]SP – Swedish National Testing and Research Institute.

ISSN 1651-9035
Report 04:13
Archive no. 35
Department of Structural Engineering and Mechanics
Concrete Structures
Chalmers University of Technology
SE-412 96 Göteborg
Sweden
Telephone: + 46 (0)31-772 1000

Cover:
Cover shows the funding agent, the participating labs, and a schematic showing the principle of the wedge-splitting test method..

Department of Structural Engineering and Mechanics
Göteborg, Sweden 2004

Application of WST-method for fracture testing of fibre-reinforced concrete

Ingemar Löfgren[I], John Forbes Olesen[II] and Mathias Flansbjer[III]
[I]Department of Structural Engineering and Mechanics, Chalmers University of Technology.

[II]DTU – Technical University of Denmark, Department of Civil Engineering, BYG.DTU.

[III]SP – Swedish National Testing and Research Institute.

ABSTRACT

To evaluate the reproducibility of the wedge-splitting test method and to provide guidelines, a round robin study was conducted in which three labs participated. The participating labs were:

- DTU –Technical University of Denmark, Department of Civil Engineering;
- CTH – Chalmers University of Technology, Department of Structural Engineering and Mechanics; and
- SP –Swedish National Testing and Research Institute.

Two different mixes were investigated; the difference between the mixes was the fibre length (Mix 1 with 40 kg of 35 mm long fibres and Mix 2 with 40 kg of 60 mm long fibres). The test results from each lab were analysed and a study of the variation was performed. From the study of the intra-lab variations, it is evident that the variations of the steel fibre-reinforced concrete properties are significant. The coefficient of variance for the splitting load was found to vary between 20 to 40%. The investigation of the inter-lab variation, based on an analysis of variance (ANOVA) indicated that there is no inter-lab variation. The test result can be said to be independent of the testing location and the equipment used (with or without *CMOD*-control).

The conclusions that can be drawn from this study are that:

- the wedge-splitting test method is a suitable test method for assessment of fracture properties of steel fibre-reinforced concrete;
- the test method is easy to handle and relatively fast to execute
- the test can be run with CMOD-control or without, in a machine with a constant cross-head displacement rate (if rate is equal to or less than 0.25 mm/min);
- due to variations in fibre distribution, the scatter of the test results is high;
- the dimensions of the specimen (height, width, and thickness) should, if possible, be four times the maximum fibre length, or at least more than three times the fibre length;
- using inverse analysis, the tensile fracture properties can be interpreted from the test result as a bi-linear stress-crack opening relationship.

Key words: Fibre-reinforced concrete, fracture testing, wedge-splitting test method, round-robin test, Nordtest.

Tillämpning av WST-metoden för provning av fiberbetong

Ingemar Löfgren[I], John Forbes Olesen[II] and Mathias Flansbjer[III]
[I]Avdelningen för konstruktion och mekanik, Chalmers tekniska högskola.

[II]DTU – Danmarks tekniska universitet.

[III]SP – Sveriges provnings och forskningsinstitut.

SAMMANFATTNING

För att utvärdera reproducerbarheten och för att utveckla metodförslag för ”kil-spräck” metoden (wedge-splitting test method) genomfördes en jämförande provning (Round-robin test) där tre laboratorier medverkade. Medverkan laboratorier var:

- DTU – Danmarks tekniska universitet, Byg.
- CTH – Chalmers tekniska högskola, avdelningen för konstruktion och mekanik.
- SP – Sveriges provnings och forskningsinstitut.

Två olika fiberbetonger undersöktes, skillnaden mellan betongerna var fiberlängden (Mix 1 med 40 kg 35 mm långa fibrer och Mix 2 med 40 kg 60 mm långa fibrer). Provningsresultaten från varje laboratorium analyserades och variansen studerades. Av resultaten från de enskilda laboratorierna framgår det att spridningen är stor för de undersökta fiberbetongerna. Varianskoefficienten, för belastningen, varierade mellan 20 och 40 %. Undersökningen av variationen mellan laboratorierna, som baserades på en analys av variansen (ANOVA), påvisade att det inte var några skillnader mellan resultaten från de olika laboratorierna. Testresultaten kan således anses vara oberoende av var och vilken utrustning som användes (med eller utan styrning mot spricköppningen).

De slutsatser som kan dras av denna undersökning är att:

- ”kil-spräck” metoden är en lämplig provningsmetod för att bestämma brottmekaniska egenskaper hos fiberbetong.
- Metoden är relativt enkel att hantera och snabb att genomföra.
- Försök kan genomföras med eller utan styrning mot spricköppningen, exempelvis i en maskin med konstant deformationshastighet (om denna kan köras med en deformationshastighet som är 0.25 mm/min eller mindre).
- På grund av variationer i fiberinnehåll är spridningen stor.
- Provkropparnas dimensioner (bredd, höjd och tjocklek) bör, om möjligt, vara fyra gånger större än den största fiberlängden (den måste minst vara tre gånger).
- Provningsresultatet kan med hjälp av inversanalys tolkas som ett bilinjärt samband mellan spänning och spricköppning.

Nyckelord: Fiberbetong, brottmekanisk provning, kil-spräck metoden, round-robin försök, Nordtest.

Contents

Preface

This report presents the results from the NORDTEST project No. 04032 (1672-04, Part I), which was started in Mars 2004 involving three labs.

The authors of this report would like to acknowledge those who have participated in this project: Eva Larsson (who participated in the testing at SP Building Technology and Mechanics), Lars Wahlström (who participated in the testing at Chalmers), Rasmus Walter (who performed the tests at DTU). Finally, Sten Hjelm at Färdig Betong is appreciated for supplying the concrete.

The financial support from the Nordtest is greatly appreciated.

Ingemar Löfgren, John Forbes Olesen, and Mathias Flansbjer

Göteborg (Sweden), Lyngby (Denmark), and Borås (Sweden), December 15, 2004.

1 Introduction

Industrialisation of the building industry is presently a very important topic, and use of fibre reinforcement as replacement for ordinary reinforcement could play an important role in this development. In some types of structures like slabs on grade, foundations and walls, fibres are likely to replace the ordinary reinforcement completely, while in other structures such as beams and slabs, fibres can be used in combination with pre-stressed or ordinary reinforcement. In both cases the potential benefits are due to economical factors, but also to rationalisation and improvement of the working environment at the construction sites. However, for this to be realised simple test methods have to be available to concrete industry. This is imperative for fibre reinforced concrete where the industry lacks such a method for their daily production quality control. This would allow concrete producers to verify and further develop their products and also provide the structural engineers with pertinent material data allowing design of structures that are safe and cost-effective. Moreover, as the design tools of the structural engineers are becoming more advanced and the design requirements more complex fracture mechanical properties are required for structural analysis. This endorses the views that there is a need for a simple and robust test method, for determining the fracture properties of fibre-reinforced cementitious composites, that can be used by small and medium large companies in their daily production without having to invest in expensive testing equipment.

During the past four decades, different methods have been proposed and used to characterize the tensile behaviour of fibre-reinforced concrete (FRC), for example by:

- measuring the flexural strength, as in the early work of Romualdi and Mandel (1964);
- determining the behaviour in terms of dimensionless toughness indices (as prescribed in ACI 544 and ASTM C 1018);
- determining the flexural toughness using the round panel test (see ASTM C 1550-2)
- determine residual flexural strengths at prescribed deflections, see Gopalaratnam & Gettu (1995), Barr et al. (1996), and RILEM TC-162 TDF (2002a).

The most recent recommendations on test methods for steel-fibre reinforced concrete (SFRC) are those by RILEM technical committee TC 162-TDF, “Test and design methods for steel fibre reinforced concrete”, see RILEM-Committee-TDF-162 (2001) and (2002a). The proposed test methods are a uniaxial tension test (UTT) and a three-point bending test (3PBT) on a notched beam. The three-point bending test on notched beams is probably the most widespread method for determining the fracture properties; see RILEM TC-50 FMC (1985) for conventional concrete and RILEM TC 162-TDF (2002) for steel fibre-reinforced concrete. The UTT requires sophisticated testing equipment, is quite time-consuming to carry out, and it has been shown that the test result is affected by machine specimen interaction; see e.g. Østergaard (2003). Drawbacks to the 3PBT are that the specimen is quite large and heavy; furthermore, the method is not suited for evaluation of material properties in existing structures. The wedge splitting test (WST) method, originally proposed by Linsbauer and Tschegg (1986) and later developed by Brühwiler and Wittmann (1990), is an interesting test method since it does not require sophisticated test equipment; the test is stable and

mechanical testing machines with a constant crosshead displacement rate can be used. Furthermore, a standard cube specimen is used, but the test can also be performed on core-drilled samples. Researchers have used the WST-method extensively, and recently there has been an increased interest in the method. The method has proved to be successful for the determination of fracture properties of ordinary concrete, at early age and later, see Østergaard (2003), and for autoclaved aerated concrete, see Trunk et al. (1999). In addition, the method has been used for the study of fatigue crack growth in high-strength concrete, see Kim and Kim (1999), and fracture behaviour of polypropylene fibre-reinforced concrete, see Elser et al. (1996). For steel fibre-reinforced concrete a small number of references can be found; Meda et al. (2001) used the WST-method (with three specimen sizes) to determine a bi-linear stress crack opening relationship through inverse analysis. Nemegeer et al. (2003) used the WST-method to investigate the corrosion resistance of cracked fibre-reinforced concrete. However, in an experimental study conducted by Löfgren (2004) it was demonstrated that horizontal cracks might develop and thus jeopardise the test; this was also shown by Leite at el. (2004). However, to the authors' knowledge no proper recommendations exist for the testing of steel fibre-reinforced concrete using the WST-method (specimen size, interpretation, etc).

The objectives of the present project were to carry out a round robin test program, with three participating labs, in order to verify the reliability of measurements and to provide guidelines for using the wedge splitting test method. The laboratories participating in this project were:

- DTU – Technical University of Denmark, Department of Civil Engineering;
- CTH – Chalmers University of Technology, Department of Structural Engineering and Mechanics; and
- SP – Swedish National Testing and Research Institute.

2 Aim

The aim of the project is to implement the wedge splitting test method as a standardised fracture test that can be used for conformity assessment and characterisation of the post-cracking behaviour of fibre-reinforced cementitious composites. The test method should be reliable, robust, simple, have a low cost and be viable to a wide range of applications; e.g. for determining early age fracture properties, and applicable to core-drilled samples.

This was achieved by investigating and verifying the wedge splitting test method in an inter-laboratory study for different types of fibre-reinforced cementitious composites. The proposed project work includes: recommendation of an appropriate test set-up and specimen size (based on previous studies) for different types of fibres.

The project relates to the construction industry as a whole but more specifically to producers of ready mix concrete, precast element manufacturers, fibre manufacturers, the authorities, and is also expected to be beneficial to companies involved in research and development of new types of fibre-reinforced cement-based composites.

3 Introduction to the Wedge-Splitting test method

In Figure 1 the specimen geometry and loading procedure are clarified. The specimen is equipped with a groove (to be able to apply the splitting load) and a starter notch (to ensure the crack propagation). Two steel platens with roller bearings are placed partly on top of the specimen partly into the groove, and through a wedging device the splitting force, F_{sp}, is applied. During a test, the load in the vertical direction, F_v, and the crack mouth opening displacement (*CMOD*) – at the same level as the splitting load is applied - is monitored.

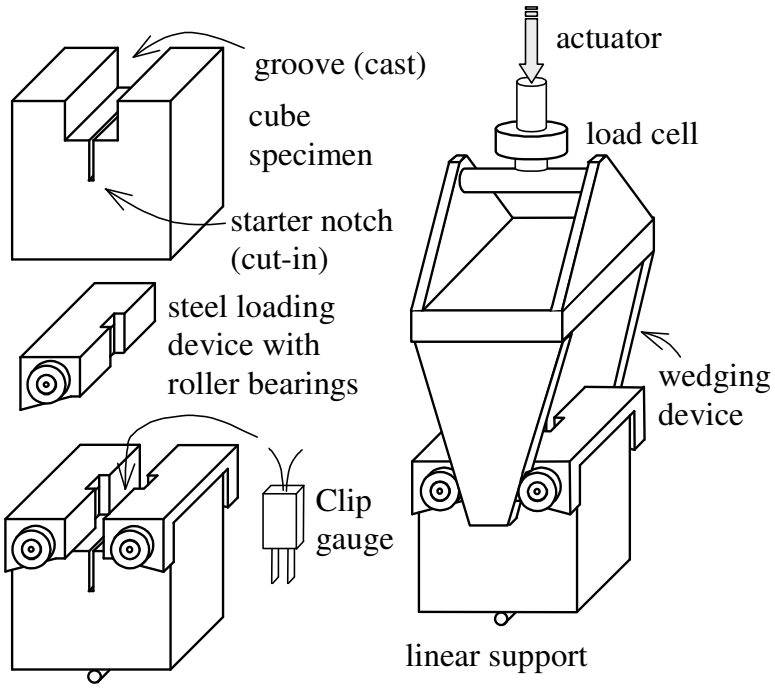

Figure 1. Schematic view of the equipment and test setup.

The applied horizontal splitting force, F_{sp}, is related to the vertical compressive load, F_v, through (see Figure 2 for notations) (eqv. 1):

$$F_{sp} = \frac{F_v}{2 \cdot \tan(\alpha)} \cdot \frac{1 - \mu \cdot \tan(\alpha)}{1 + \mu \cdot \cot(\alpha)} \approx 1.866 \cdot F_v \qquad \text{(eqv. 1)}$$

were α is the wedge angle (here $\alpha = 15$ degrees), and μ is the coefficient of friction for the roller bearing. The coefficient of friction normally varies between 0.1 and 0.5 %. The resulting effect on the splitting force, F_{sp}, is about 0.4 to 1.9 %, see RILEM Report 5 (1991).

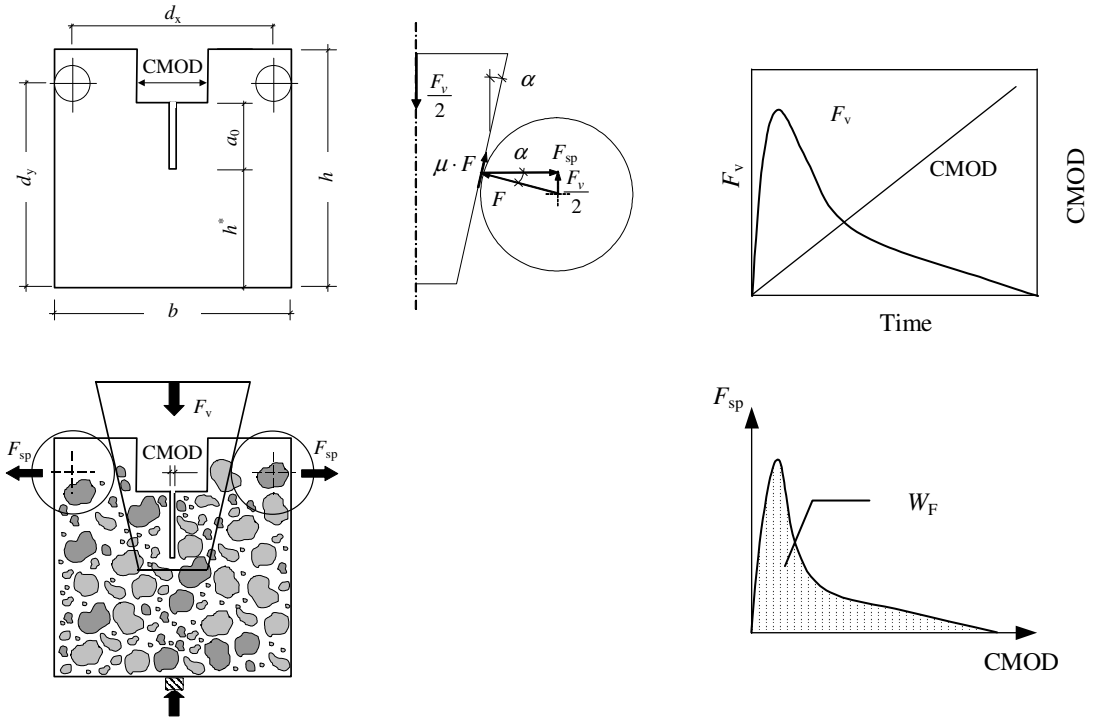

Figure 2. The principle of the WST method, specimen geometry and evaluation of the work of fracture, W_F.

In the WST no measurements are made of the real crack opening – this is often due to measurement technique or due to specific test conditions. As can be seen in Figure 3, while the *CMOD* is measured at some distance from the tip of the notch the *CTOD* is the crack opening at the tip of the notch. The crack tip opening displacement (*CTOD*), however, represents a 'true' crack opening and, thus, is an important parameter when evaluating the fracture properties. Relationships between the *CMOD* and the crack tip opening displacement (*CTOD*) have been evaluated with the aid of FE-analyses, see Figure 4 and Figure 5, of test results on five different mixes.

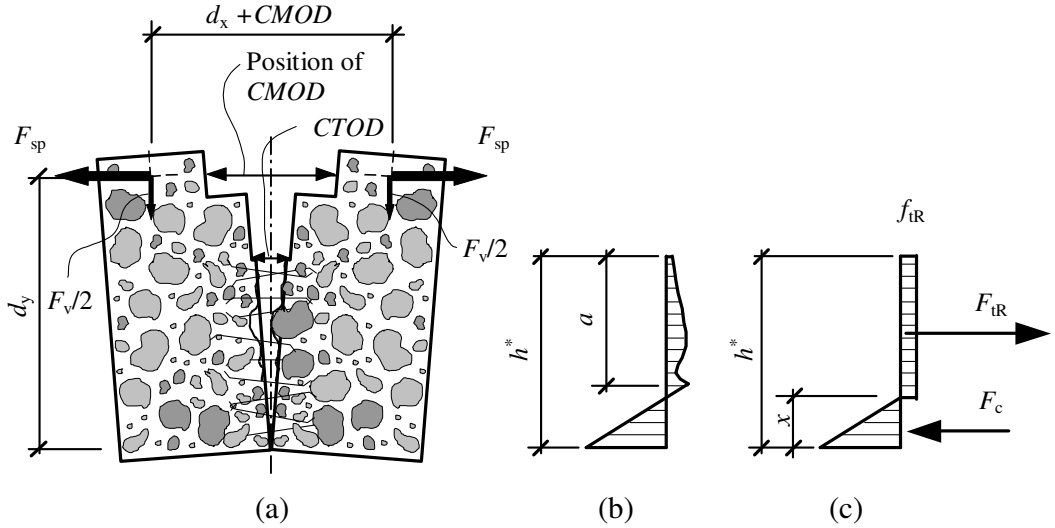

Figure 3. *(a) Schematic view of a cracked specimen and the definition of CMOD and CTOD. (b) The stress distribution in a cracked WST-specimen (h^* denotes the total length of the ligament and a the length of the fictitious crack). (c) Simplified stress distribution based on the assumption of a constant residual tensile stress f_{tR}. x denotes the height of the compressive zone, d_x the distance (for the undeformed specimen) between the loading points, and d_y the distance from the bottom of the specimen to the point where the splitting load is applied (for the undeformed specimen).*

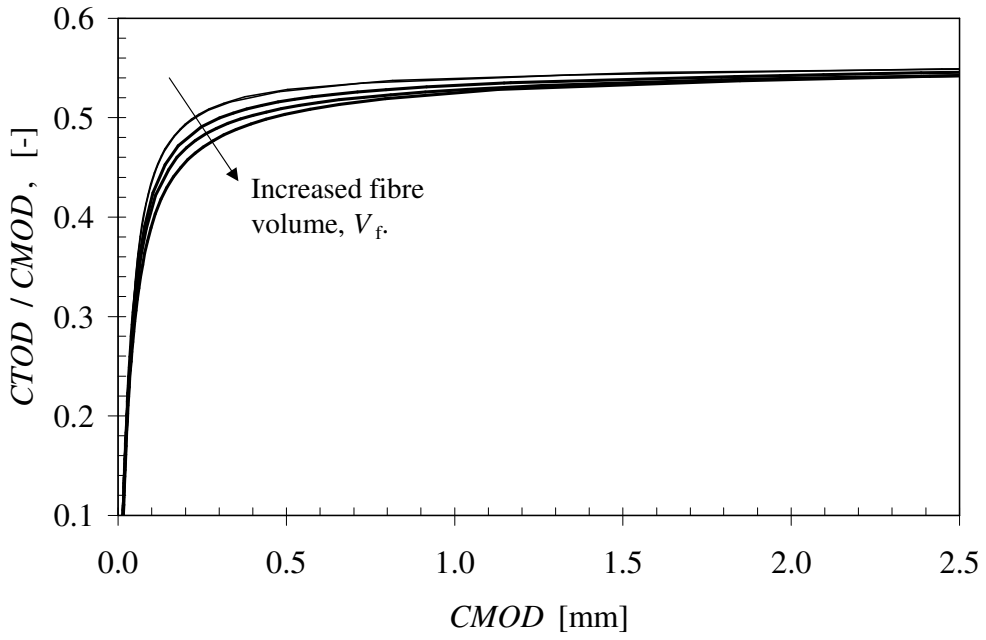

Figure 4. *Relationship between CTOD and CMOD for WST-specimens with a cube size of 150×150 mm^2.*

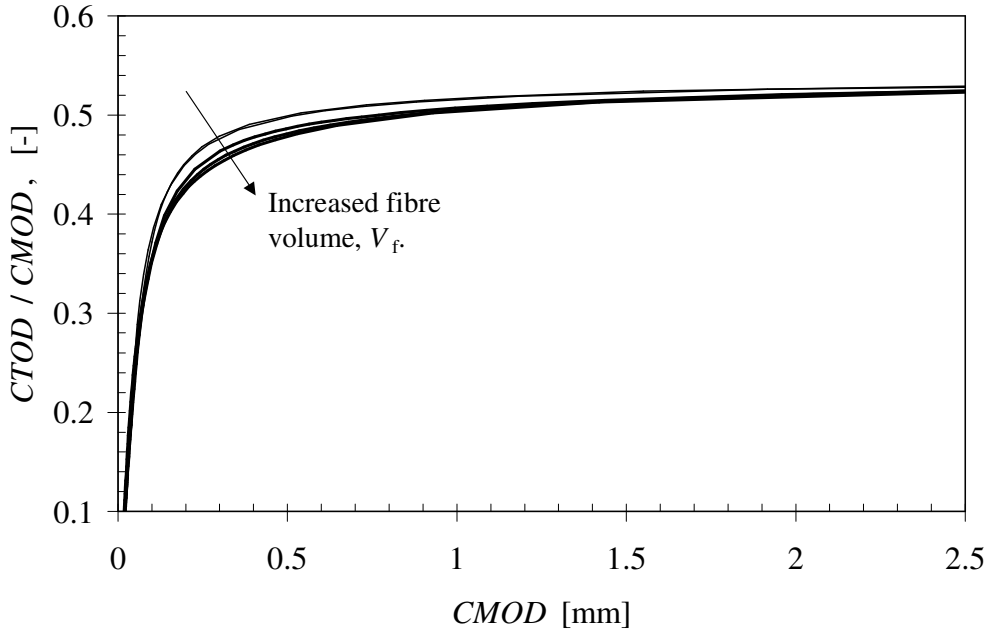

Figure 5. Relationship between CTOD and CMOD for WST-specimens with a cube size of 200×200 mm^2.

For the 150×150 mm^2 WST-specimens, the following expression (based on five mixes with the fibre content varying between 0.5% and 1.0 %) has been evaluated for the relationship between the *CMOD* and the *CTOD* (eqv. 2):

$$CTOD = 0.551 \cdot CMOD - 0.0084 \text{ [mm]} \quad \text{(eqv. 2)}$$

For the 200×200 mm^2 WST-specimens, the following expressions have been evaluated for the relationship between the *CMOD* and the *CTOD* (eqv. 3):

$$CTOD = 0.533 \cdot CMOD - 0.0110 \text{ [mm]} \quad \text{(eqv. 3)}$$

At a specific *CMOD* the energy dissipated during fracture, W_{fCMOD}, is normalised with respect to the total ligament area, A_{lig}, at complete fracture. This intermediate, specific fracture energy is denoted G_{fCMOD} [Nm/m^2], and may be determined directly from the test result by performing the calculation specified in (eqv. 4):

$$G_{fCMOD} = \frac{W_{fCMOD}}{A_{lig}} \quad \text{(eqv. 4)}$$

where, W_{fCMOD} is the area under the splitting load-*CMOD* curve and A_{lig} is the area of the ligament (all of the expected total cracked area).

However, as the main benefit from fibre reinforcement is the ability to transfer stress across a crack it is important to characterise the stress-crack opening relationship. For this, inverse analysis has proven to be successful to determine the non-linear fracture mechanics parameters from the experimental result. Inverse analysis – also refereed to as parameter or function estimation – is achieved by minimizing the differences

between calculated displacements and target displacements obtained from test results (e.g. *CMOD*), see Figure 6. In this manner, inverse analysis can be used to determine a σ-w relationship from test results of methods like the three point bending test on notched beams and the WST. The stress-crack opening relationship can either be approximated as bilinear or non-linear. For regular concrete (i.e. without fibres), extensive research has been carried out to determine the best approach for inverse analysis and different strategies have been proposed. Of the available approaches, some define the shape of the σ-w relationship as bi-linear – see e.g. Roelfstra and Wittmann (1986), Trunk et al., 1999, Planas et al. (1999), Østergaard et al., 2002, Østergaard (2003), Bolzon et al. (2002), and Que and Tin-Loi (2002) – while in others a poly-linear σ-w relationship is used in conjunction with a stepwise analysis – see e.g. Kitsutaka (1997), Nanakorn and Horii (1996). Some methods have also been used for FRC; see e.g. Uchida et al. (1995), Kooiman (2000), Meda et al. (2001), Sousa et al. (2002), and Löfgren et al. (2004).

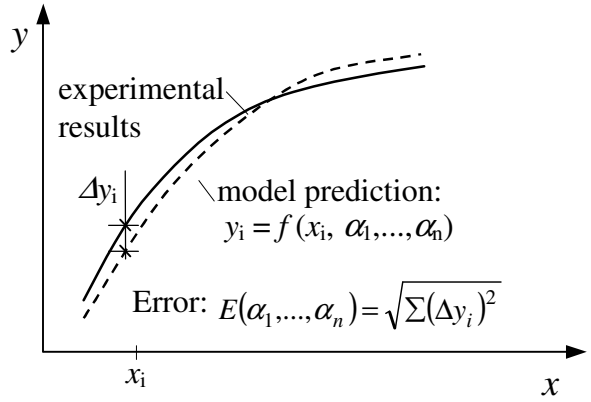

Figure 6. Principle of inverse analysis.

A simplified approach to determine a residual tensile stress is to use the given relationships between *CMOD* and *CTOD* (eqv. 2 & 3) and an assumption of the height of the compressive zone. It is then possible to determine the residual tensile stress, f_{tR}, at a specific *CMOD* and calculate the corresponding crack opening. Figure 3(b) shows the non-linear stress distribution in a cracked WST-specimen. If this is simplified according to Figure 3(c), assuming a constant residual tensile stress f_{tR}, and that the height of the compressive zone is given by (eqv. 5):

$$x \approx \frac{h^*}{10} \qquad \text{(eqv. 5)}$$

then the residual tensile stress, f_{tR} can be calculated by solving the equilibrium equation of forces (eqv. 6) and the equilibrium equation of moment with respect to the position of the neutral axis (eqv. 7):

$$F_{tR} - F_c - F_{sp} = 0 \Leftrightarrow F_c = F_{tR} - F_{sp} \qquad \text{(eqv. 6)}$$

$$F_{tR} \cdot \left(\frac{h^* - x}{2} \right) + F_c \cdot \left(\frac{2}{3} x \right) - F_{sp} \left(d_y - x - \frac{(CMOD/2)^2}{d_y - x} \right) - \frac{F_v}{2} \left(\frac{d_x + CMOD}{2} \right) = 0 \qquad \text{(eqv. 7)}$$

4 Materials and specimen Preparation

4.1 Concrete mix

In this study all specimens were manufactured at one location and then shipped to the participating laboratories. Two different mixes were investigated and for each lab six specimens were prepared, a total of 18 specimens, for each mix. The concrete used in this investigation was a self-compacting concrete, with a water cement ratio (w/c) of 0.55 and a fibre content of 40 kg/m^3 (fibre type Dramix, from Bekaert). Two mixes were made with two different fibre lengths; see Table 1 for mix composition. In Mix 1 the fibre length was 35 mm and in Mix 2 the fibre length was 60 mm. The concrete was produced and delivered from a ready-mix concrete company, AB Färdig Betong. At the concrete plant, one cubic meter was mixed in the mixer and the fibres were added as the concrete was tipped into the truck. In the truck, the concrete and the fibres were mixed for five minutes to ensure a good dispersion. In this way the fibres were distributed relatively uniformly in the mix. The air content was measured at the plant taking out 20 litre of concrete from the truck and a washout test was performed on the concrete used to determine the amount of fibres within the mix. Only one sample was taken so it is likely that it is not representative but it gives an indication.

After casting, the specimens were covered with plastic and stored in a climate room with a constant temperature of 20ºC and relative humidity of 65%. The specimens were shipped after two weeks to the participating labs where they were stored in water until the time of testing which in most cases took place 28 days after casting. One week prior to testing the notches were prepared by using a wet diamond saw.

Table 1. Concrete mix compositions.

Constituents	**Density** [kg/m^3]	**Mix 1** [kg/m^3]	**Mix 2** [kg/m^3]
CEM II/A-LL 42.5 R	3100	350	350
Filler, micro glass	2500	80	80
Water	1000	189	189
w/c-ratio	-	0.55	0.55
Plasticizer, Sikament 56	1090	0.4	0.953
Aggregates:			
00 – 08 mm	2535	971.76	971.76
08 – 16 mm	2637	667.40	667.40
Fibres, kg (V_f)	7800	40 (0.51%)	40 (0.51%)
(Aspect ratio/Length)		(65/35)	(65/60)
Measured fibre content [kg/m^3] *:		31.5	36.9
Measured air content* :		8.9%	10.8%

*measured at the concrete plant, 20 litres of concrete was taken out at the back of the truck.

Standard cube specimens (150×150×150 mm^3) were also prepared for testing of the compressive strength and the splitting tensile strength. The splitting tensile test, however, cannot be directly applied to determine the tensile strength of fibre-reinforced concrete as the fibres increase the ductility and thus alters the factor (usually 0.8 to 0.9) relating the tensile and the splitting strength, see also Olesen et al. (2003). The result from the compressive strength tests can be seen in Table 2 while the results from the splitting tensile strength tests can be viewed in Table 3. From the results it appears that

Mix 2 resulted in slightly higher compressive and splitting tensile strengths (the ratios are 1.15 for the compressive strength and 1.25 for the splitting tensile strength). The reason for this is believed to be due to differences in porosity (air content) where the shorter fibres seem to produce and entrap more air than the longer fibres.

Table 2. Results from compressive strength tests on 150×150×150 mm^3 cube specimens.

Mix 1		**Mix 2**	
Specimen	Compressive strength [MPa]	Specimen	Compressive strength [MPa]
1	27.0	1	31.0
2	26.7	2	31.3
3	27.3	3	31.1
Average:	27.0	Average:	31.1
Cov [%]:	1.11%	Cov [%]:	0.49%

Table 3. Results from splitting tensile strength tests on 150×150×150 mm^3 cube specimens.

Mix 1		**Mix 2**	
Specimen	Splitting tensile strength [MPa]	Specimen	Splitting tensile strength [MPa]
1	1.73	1	2.57
2	2.40	2	2.69
3	2.43	3	2.93
Average:	2.19	Average:	2.73
Cov [%]:	18.10%	Cov [%]:	6.71%

4.2 Specimens

In this study two different specimen sizes were used, see Figure 7. For the shorter fibre (35 mm long) a 150×150 mm^2 specimen was used while for the longer fibre (60 mm long) a 200×200 mm^2 specimen was used. Both specimen sizes had a thickness of 150 mm and were equipped with 25 mm deep guide notches (see Figure 7). The specimens were cast in specially prepared formwork made out of plywood, see Figure 8 and Figure 9.

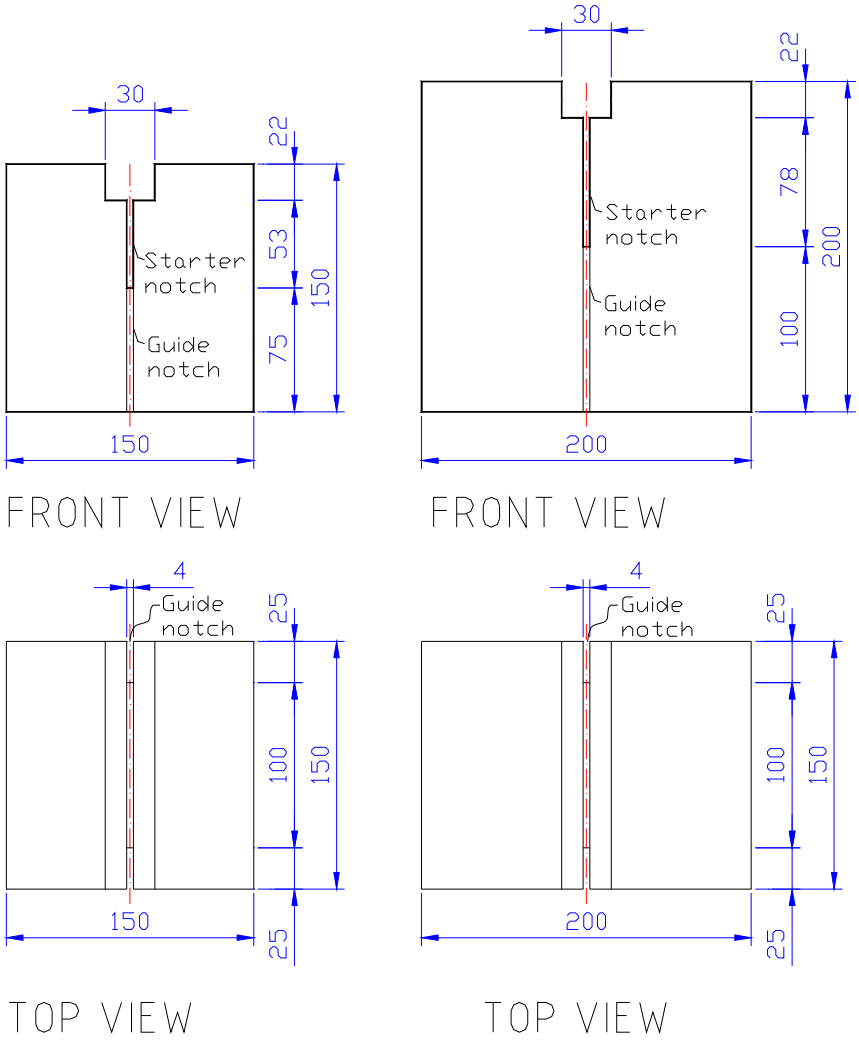

Figure 7. *Specimen geometries: (a) 150×150 mm^2 specimens used for concrete Mix 1 (35 mm long fibres); and (b) 200×200 mm^2 specimens used for concrete Mix 2 (60 mm long fibres).*

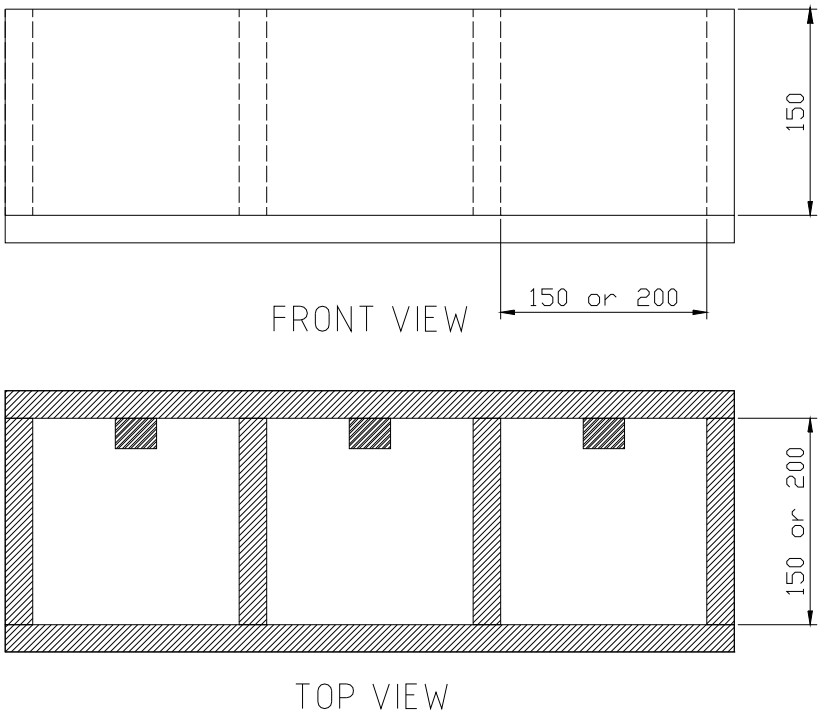

Figure 8. Formwork used for the specimens.

Figure 9. Casting the specimens.

5 Tests performed at the laboratories

5.1 Specified test procedure

The testing system consists of: frame, actuator, load cell, clip gauge (or other measuring device), controller and data acquisition equipment as a minimum. It is preferable to have a closed-loop controlled machine, however, this is not required. The load shall be measured with an accuracy of ±1% of the maximum load value in the test. The accuracy of the displacement-measuring device, measuring the CMOD, shall be better than ±0.01 mm. The specimens may be removed from the water 60 minutes prior to starting the test. The specimen is then placed in the testing machine and should be pre-loaded to a level of 50 to 100 N before. Thereafter the test can begin and the testing machine should be operated so that, in the beginning of the test, the measured *CMOD* increases at a constant rate of 25 to 50 μm/min for *CMOD* ranging from 0 to 0.2 mm. For *CMOD* values between 0.2 and 2 mm a constant rate of 0.25 mm/min should be applied. When the *CMOD* is larger than 2 mm, the rate of loading may be increased to 0.5 mm/min. The changes in the loading rate should be made progressively in such a way that it influences the test result minimally – i.e. the changes should not be too abrupt as this may result in a sudden increase in the load.

The load-*CMOD* diagram is determined by continuously measuring and logging corresponding values of the vertical load, F_v, and the *CMOD*. During the first two minutes, data shall be logged with a frequency not less than 5 Hz; thereafter, until the end of the test, the frequency shall not be less than 1 Hz.

For the test to be valid it is required that the load-*CMOD* response is stable. After the test, the height, *h*, and the thickness, *l*, of the ligament is to be measured with an accuracy of ±0.1 mm, see Figure 10.

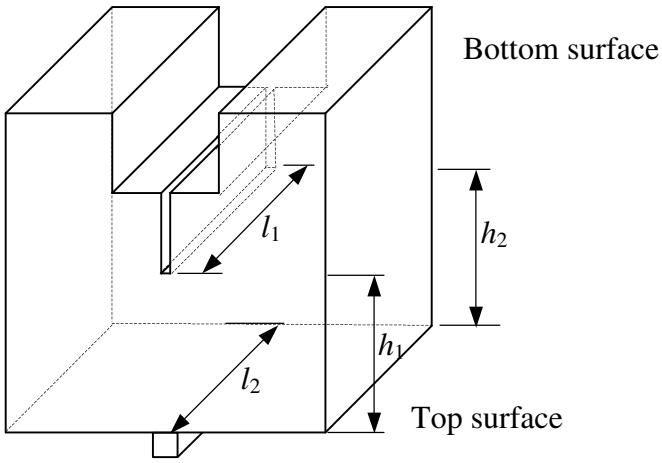

Figure 10. Definition of dimensions to be measured.

5.2 Tests conducted at CTH

The tests were performed in a deformation controlled testing machine (screw driven), see Figure 11. The initial rate of the vertical displacement was approximately 0.25 mm/min, which resulted in a CMOD-rate of 25 to 50 μm/min before cracking was initiated. As the crack was propagating the CMOD-rate increased until it stabilised at a constant rate of 0.2 mm/min. The crack mouth opening (CMOD) was measured with a MTS clip gauge (gauge length 10 mm and maximum travel 5 mm), placed in the groove. In addition, the horizontal deformation at the centre of the roller bearings was measured with two LVDT-gauges (type D2/200A/256 from RDP Group UK) with a stroke of ±5mm and an accuracy better than ±0.1 %. The vertical deformation was measured with an LVDT-gauge. In the tests, a wedge angle of 15° was used and the roller bearings used were of the double row, deep groove type from SKF (designation 4205 ATN9).

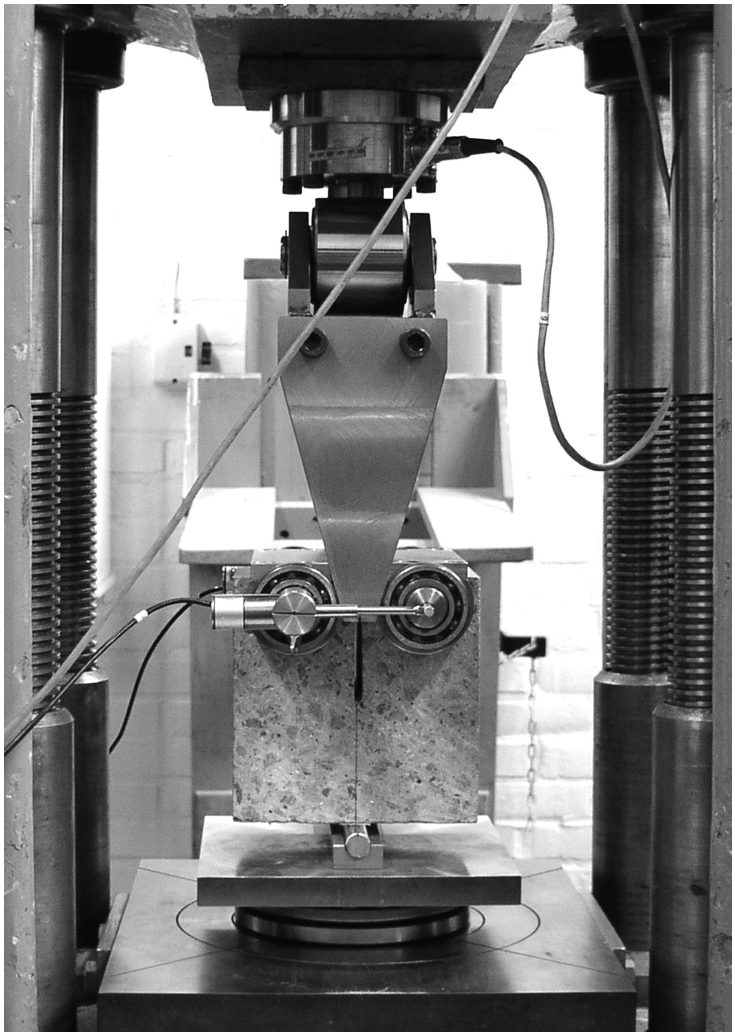

Figure 11. Experimental setup used at CTH.

The individual specimen dimensions for the 150×150 mm^2 specimens can be seen in Table 4 and the results (splitting load-CMOD curve) can be seen in Figure 12. For the 200×200 mm^2 specimens, the individual specimen dimensions can be seen in Table 5 and the results (splitting load-CMOD curve) can be seen in Figure 13.

Table 4. Individual dimensions of the 150×150 mm^2 specimens tested at CTH.

WST	Weight	Dimension				Area ligament
		h_1	h_2	l_1	l_2	$A_{lig} = h_{averae}$ x $l_{average}$
[no]	[kg]	[mm]	[mm]	[mm]	[mm]	[mm^2]
1-1	6.900	76.5	76.8	99.2	98.8	7586.6
1-2	6.945	77.0	76.6	99.0	97.7	7547.9
1-3	6.885	76.5	77.0	99.8	99.5	7646.0
1-4	6.902	77.1	76.6	99.4	98.8	7617.5
1-5	6.957	76.0	76.6	100.2	98.9	7594.5
1-6	6.880	76.8	76.5	99.5	99.1	7615.9
Average	6.912	76.6	76.7	99.5	98.8	7601.4
stdv	0.0320	0.40	0.16	0.43	0.60	33.41
COV	0.46%	0.52%	0.20%	0.43%	0.61%	0.44%

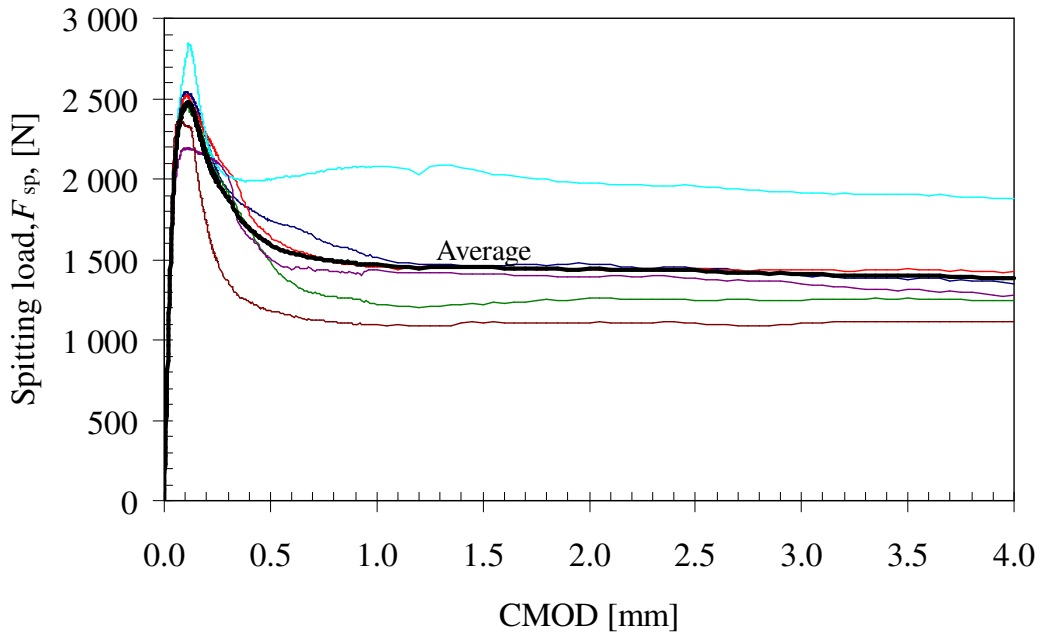

Figure 12. Splitting load-CMOD curve for the 150×150 mm^2 specimens tested at CTH (Mix 1, 40 kg of 35 mm long fibres).

Table 5. Individual dimensions of the 200×200 mm^2 specimens tested at CTH.

WST	Weight	Dimension				Area ligament
		h_1	h_2	l_1	l_2	$A_{lig} = h_{averae} \times l_{average}$
[no]	[kg]	[mm]	[mm]	[mm]	[mm]	[mm^2]
1-1	12.752	100.5	99.6	99.5	98.5	9905.0
1-2	12.603	99.8	99.5	99.8	95.5	9730.3
1-3	12.628	99.8	99.5	100.0	98.2	9873.8
1-4	12.512	100.1	99.6	100.2	98.7	9927.6
1-5	12.558	99.9	99.7	100.1	98.9	9925.6
1-6	12.670	99.9	99.7	99.8	98.7	9905.7
Average	12.621	100.0	99.6	99.9	98.1	9878.0
stdv	0.085	0.250	0.081	0.230	1.288	74.9
COV	0.67%	0.25%	0.08%	0.23%	1.31%	0.76%

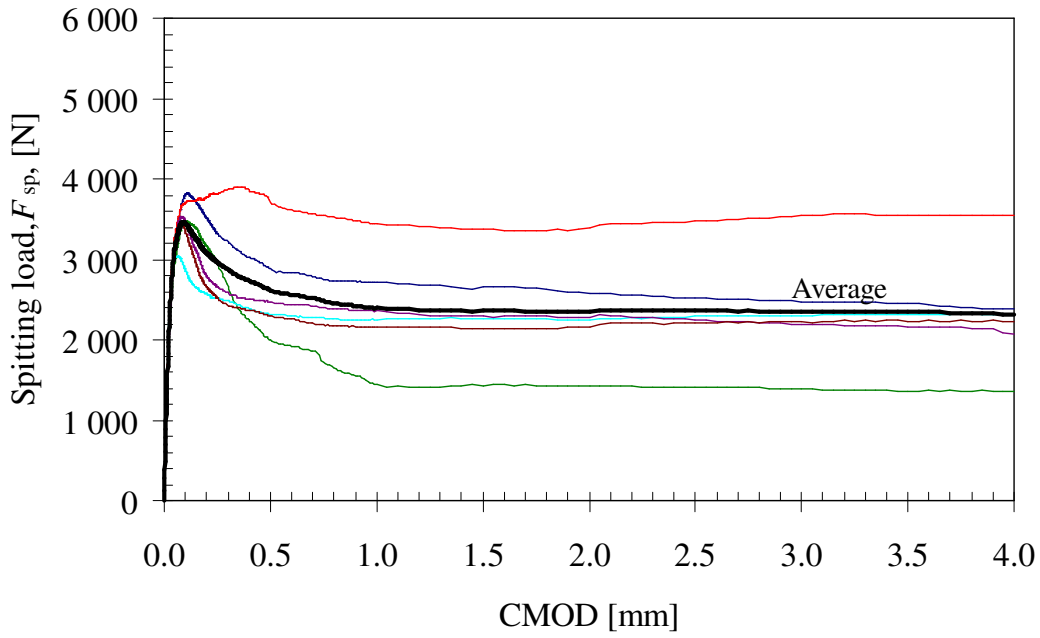

Figure 13. Splitting load-CMOD curve for the 200×200 mm^2 specimens tested at CTH (Mix 2, 40 kg of 60 mm long fibres).

5.2.1 Investigation of the effects of a guide notch

In addition to the round robin test program, an investigation of the effects of the guide notch was conducted. In an earlier investigation (see Löfgren 2004) it was found that for steel-fibre reinforced concrete, with a fibre content above 0.5%, there were some problems with horizontal cracks in some specimens. In another investigation (see Löfgren et al. 2004) it was shown that the use of a guide notch prevents this type of cracks. Hence, as part of this NORDTEST project it was decided to do a comparison between the fracture properties for specimens with a guide notch and specimens without a guide notch, and to study the influence on the scatter of the test result.

For this study, twelve specimens, with the dimensions 200×200×150 mm^3, were prepared using Mix 1 (40 kg of 35 mm long fibres). Six of the specimens were equipped with guide notches while the remaining specimens were cut to a thickness of 100 mm (25 mm were cut from each side of the specimen), see Figure 14.

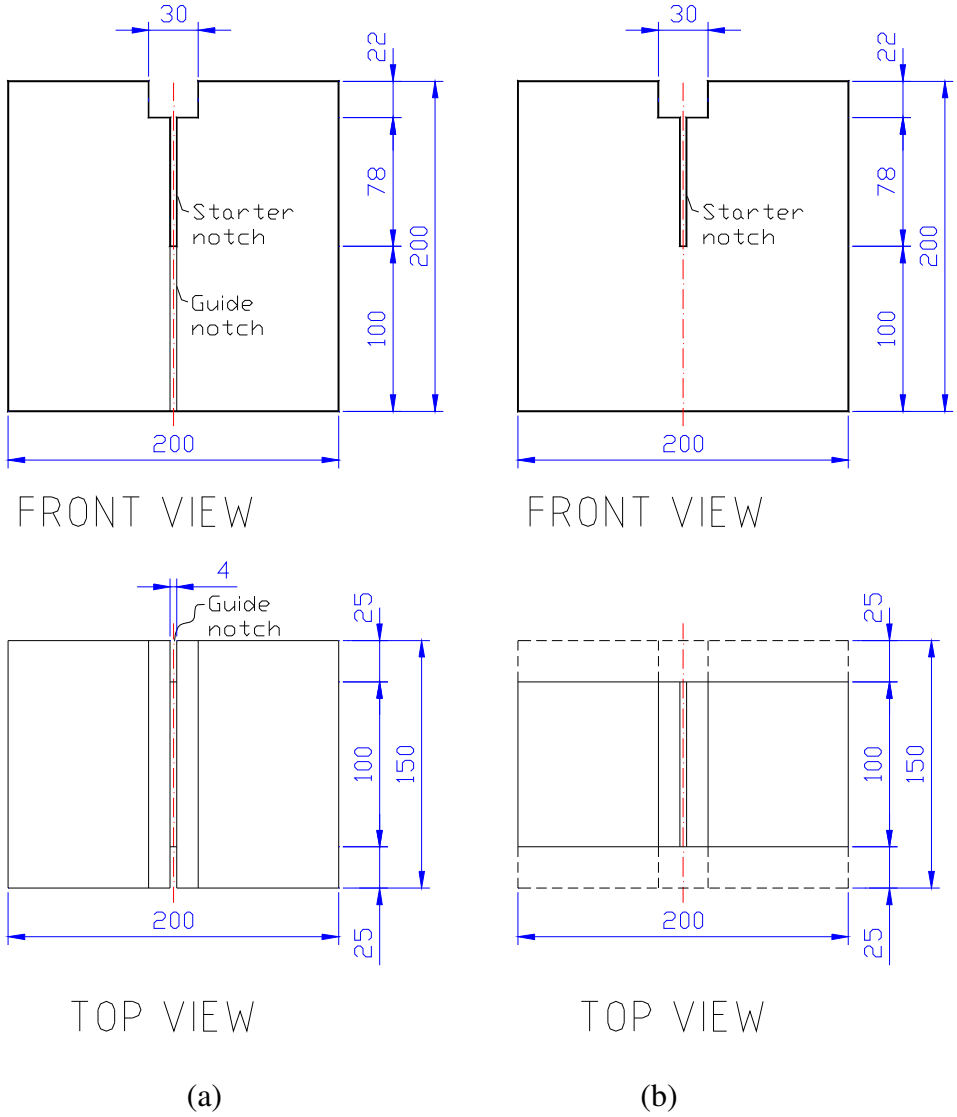

Figure 14. (a) Specimens with guide notch (GN) 200×200×150 mm^3 (Mix 2, 40 kg of 35 mm long fibres). (b) Specimens with only starter notch (SN) 200×200×100 mm^3 (Mix 1, 40 kg of 35 mm long fibres).

The individual specimen dimensions for the specimens with guide notch can be seen in Table 6 and the results (splitting load-CMOD curve) can be seen in Figure 15. For the specimens without guide notch, the individual specimen dimensions can be seen in Table 7 and the results (splitting load-CMOD curve) can be seen in Figure 16.

Table 6. Individual dimensions of the 200×200 mm^2 specimens with a guide notch.

WST	Weight	Dimension				Area ligament
		h_1	h_2	l_1	l_2	$A_{lig} = h_{averae} \times l_{average}$
[no]	[kg]	[mm]	[mm]	[mm]	[mm]	[mm^2]
1-1	12.854	100.0	99.6	98.8	97.1	9777.4
1-2	12.736	100.1	99.5	99.3	97.2	9805.9
1-3	12.692	100.1	99.6	98.9	97.6	9810.3
1-4	12.837	100.1	99.5	97.5	96.8	9698.1
1-5	12.733	99.8	98.1	98.1	97.5	9679.8
1-6	12.832	99.6	97.0	97.0	96.8	9525.8
Average	12.781	99.9	98.9	98.3	97.2	9716.2
stdv	0.0683	0.210	1.088	0.887	0.339	108.2
COV	0.53%	0.21%	1.10%	0.90%	0.35%	1.11%

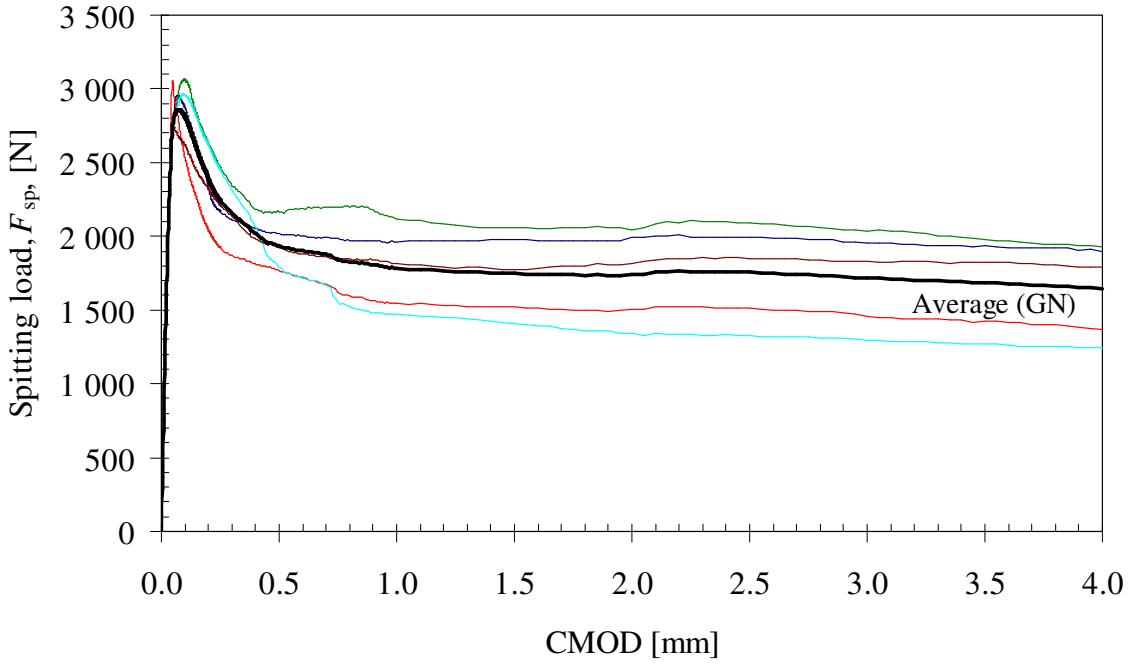

Figure 15. Splitting load versus CMOD for the 200×200 mm^2 specimens with a guide notch (Mix 1, 40 kg of 35 mm long fibres).

Table 7. Individual dimensions of the 200×200 mm² specimens without a guide notch.

WST	Weight	Dimension				Area ligament
		h_1	h_2	l_1	l_2	$A_{lig} = h_{averae} \times l_{average}$
[no]	[kg]	[mm]	[mm]	[mm]	[mm]	[mm²]
1-1	8.567	100.8	100.3	101.1	100.0	10108.5
1-2	8.469	100.4	100.4	99.9	99.2	9991.3
1-3	8.470	100.6	100.1	100.2	98.9	9989.8
1-4	8.454	99.7	101.1	99.9	99.4	9999.4
1-5	8.637	99.9	100.6	102.4	100.8	10183.4
1-6						
Average	8.519	100.3	100.5	100.7	99.7	10054.5
stdv	0.0796	0.482	0.357	1.070	0.759	87.7
COV	0.93%	0.48%	0.36%	1.06%	0.76%	0.87%

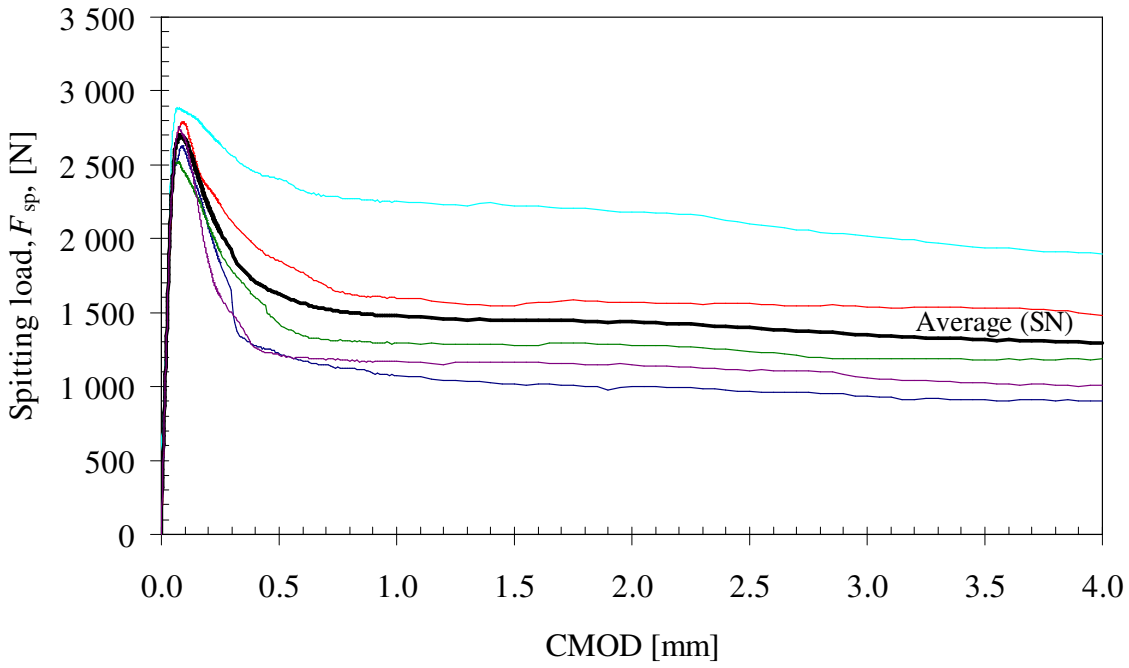

Figure 16. Splitting load versus CMOD for the 200×200 mm² specimens without a guide notch (Mix 1, 40 kg of 35 mm long fibres).

5.3 Tests conducted at DTU

The tests were performed under *CMOD* control in an Instron 6025 universal testing machine with a capacity of 100 kN. The *CMOD* was measured with an Instron clip gauge, gauge length 10 mm and maximum travel 5 mm. In the tests, a wedge angle of 15° was used and the roller bearings used were of the double-row-deep-groove type (manufactured by SKF, designation 4203 ATN9), see Figure 17 for the experimental setup.

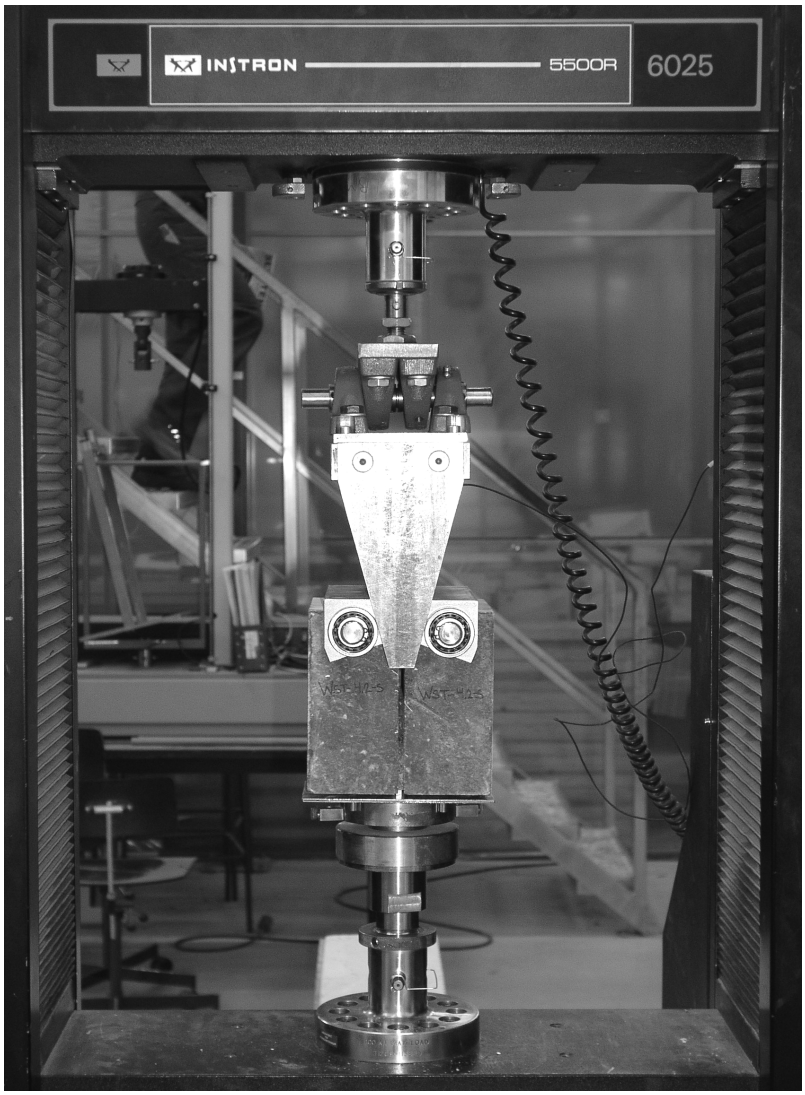

Figure 17. Experimental setup used at DTU.

The individual specimen dimensions for the 150×150 mm^2 specimens can be seen in Table 8 and the results (splitting load-CMOD curve) can be seen in Figure 18. For the 200×200 mm^2 specimens, the individual specimen dimensions can be seen in Table 9 and the results (splitting load-CMOD curve) can be seen in Figure 19.

Table 8. Individual dimensions of the 150×150 mm^2 specimens tested at DTU.

WST	Weight	Dimension				Area ligament
		h_1	h_2	l_1	l_2	$A_{lig} = h_{averae} \times l_{average}$
[no]	[kg]	[mm]	[mm]	[mm]	[mm]	[mm^2]
1-1						
1-2	6.680	75.0	75.0	100.5	99.5	7500.0
1-3	6.610	75.0	75.0	100.0	100.0	7500.0
1-4	6.530	75.0	74.0	101.0	100.5	7505.9
1-5	6.620	74.0	74.5	102.5	102.0	7592.1
1-6						
Average	6.610	74.8	74.6	101.0	100.5	7524.5
stdv	0.0616	0.500	0.479	1.080	1.080	45.1
COV	0.93%	0.67%	0.64%	1.07%	1.07%	0.60%

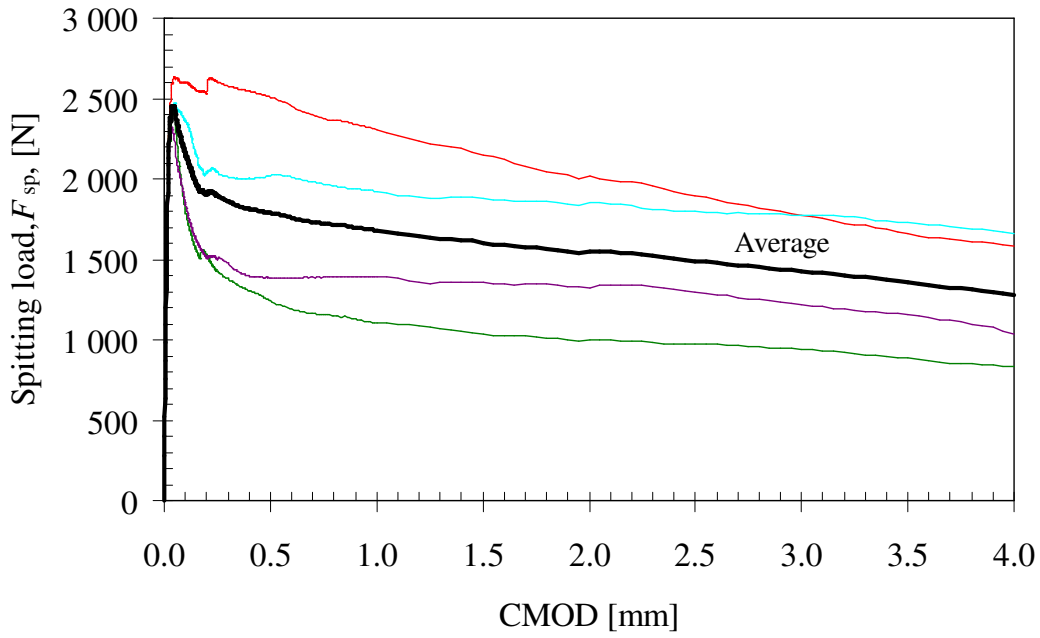

Figure 18. Splitting load-CMOD curve for the 150×150 mm^2 specimens tested at DTU (Mix 1, 40 kg of 35 mm long fibres).

Table 9. Individual dimensions of the 200×200 mm^2 specimens tested at DTU.

WST	Weight	Dimension				Area ligament
		h_1	h_2	l_1	l_2	$A_{lig} = h_{averae} \times l_{average}$
[no]	[kg]	[mm]	[mm]	[mm]	[mm]	[mm^2]
1-1	12.500	97.0	98.0	100.0	100.0	9750.0
1-2	12.260	99.0	100.0	98.5	99.0	9825.6
1-3	12.340	99.5	99.5	100.0	100.0	9950.0
1-4	12.280	99.0	99.0	101.5	102.5	10098.0
1-5	12.520	99.5	99.5	100.0	100.5	9974.9
1-6	12.200	100.0	100.0	101.5	102.0	10175.0
Average	12.350	99.0	99.3	100.3	100.7	9962.3
stdv	0.1319	1.049	0.753	1.129	1.329	159.8
COV	1.07%	1.06%	0.76%	1.13%	1.32%	1.60%

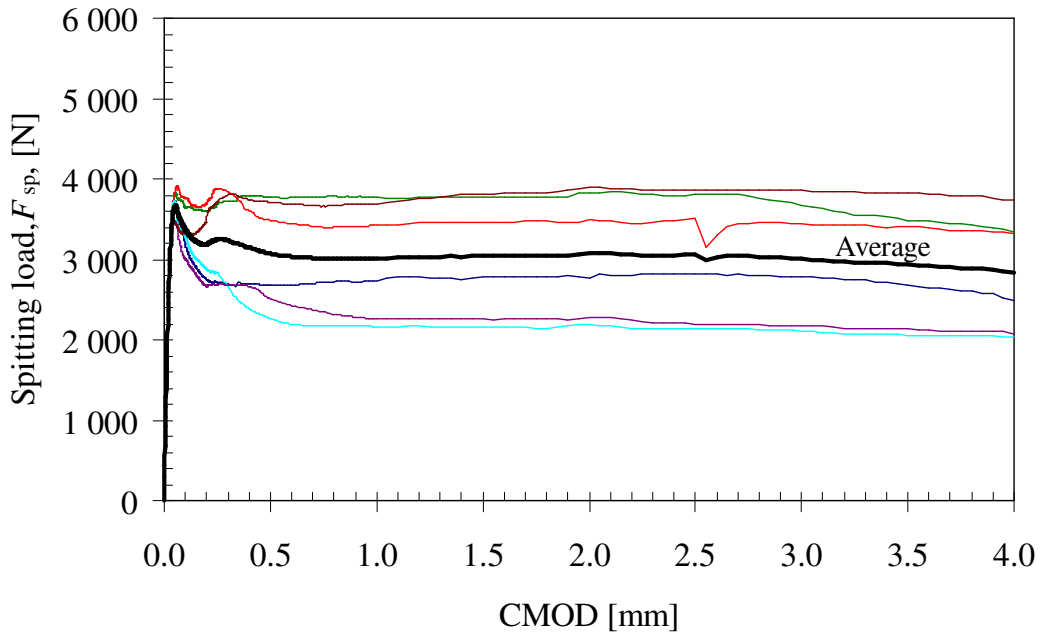

Figure 19. Splitting load-CMOD curve for the 200×200 mm^2 specimens tested at DTU (Mix 2, 40 kg of 60 mm long fibres).

5.4 Tests conducted at SP

The tests were performed under *CMOD* control in an Instron 8501 universal testing machine with a capacity of 25 kN. The *CMOD* was measured with an Instron clip gauge 2670-116, gauge length 10 mm and maximum travel 4 mm. In the tests, a wedge angle of 15° was used and the roller bearings used were of the double-row-deep-groove type (manufactured by SKF, designation 4203 ATN9), see Figure 20 for the experimental setup.

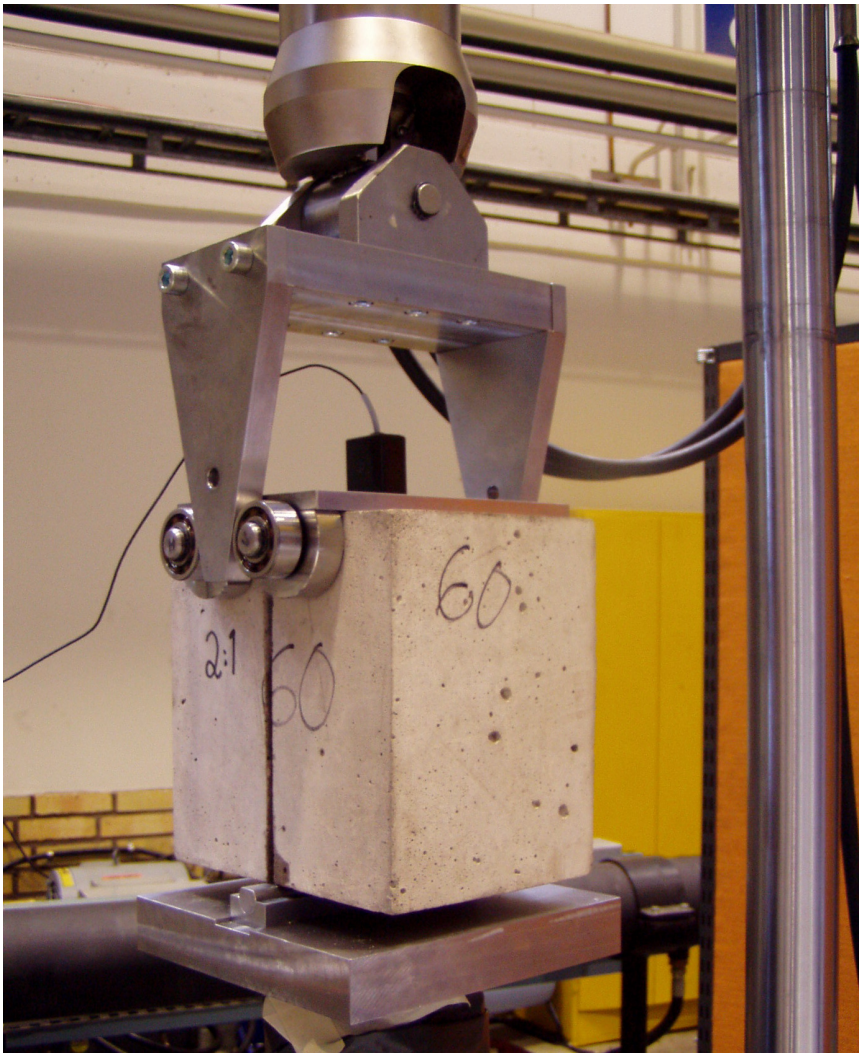

Figure 20. Experimental setup used at SP.

The individual specimen dimensions for the 150×150 mm^2 specimens can be seen in Table 10 and the results (splitting load-CMOD curve) can be seen in Figure 21. For the 200×200 mm^2 specimens, the individual specimen dimensions can be seen in Table 11 and the results (splitting load-CMOD curve) can be seen in Figure 22.

Table 10. Individual dimensions of the 150×150 mm^2 specimens tested at SP.

WST	Weight	Dimension				Area ligament
		h_1	h_2	l_1	l_2	$A_{lig} = h_{averae} \times l_{average}$
[no]	[kg]	[mm]	[mm]	[mm]	[mm]	[mm^2]
1-1	6.964	75.8	76.4	97.9	98.9	7488.2
1-2	6.937	76.7	77.2	98.5	99.7	7625.7
1-3	6.932	74.9	74.9	98.1	98.4	7358.9
1-4	6.957	76.6	76.6	98.7	99.3	7583.4
1-5	6.949	74.8	74.8	97.6	98.3	7326.7
1-6	6.947	75.7	75.7	99.5	99.8	7543.5
Average	6.948	75.8	75.9	98.4	99.1	7487.7
stdv	0.0120	0.807	0.967	0.677	0.641	121.5
COV	0.17%	1.07%	1.27%	0.69%	0.65%	1.62%

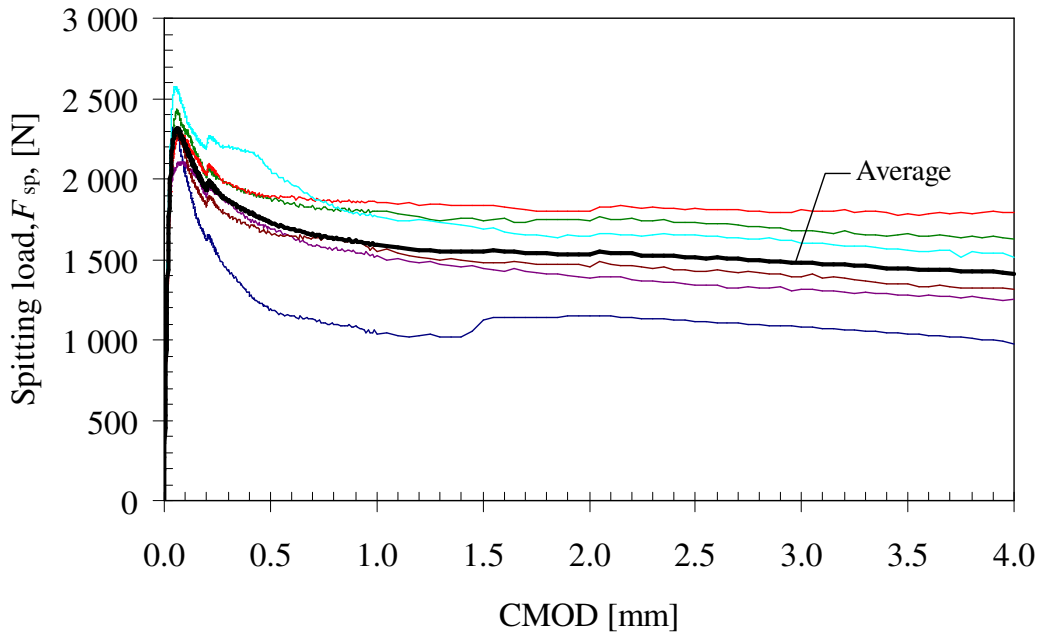

Figure 21. Splitting load-CMOD curve for the 150×150 mm^2 specimens tested at SP (Mix 1, 40 kg of 35 mm long fibres).

Table 11. Individual dimensions of the 200×200 mm² specimens tested at SP.

WST	Weight	Dimension				Area ligament
		h_1	h_2	l_1	l_2	$A_{lig} = h_{averae} \times l_{average}$
[no]	[kg]	[mm]	[mm]	[mm]	[mm]	[mm²]
1-1	12.643	99.4	100.4	99.2	100.4	9970.0
1-2	12.770	99.7	100.0	98.2	98.9	9840.2
1-3	12.826	99.6	100.0	97.4	98.1	9755.5
1-4	12.678	99.6	100.5	98.3	99.4	9889.9
1-5	12.547	99.4	100.0	99.2	100.4	9950.1
1-6	12.792	99.6	100.0	98.5	99.4	9875.2
Average	12.709	99.6	100.2	98.5	99.4	9880.2
stdv	0.1057	0.122	0.235	0.680	0.887	77.8
COV	0.83%	0.12%	0.23%	0.69%	0.89%	0.79%

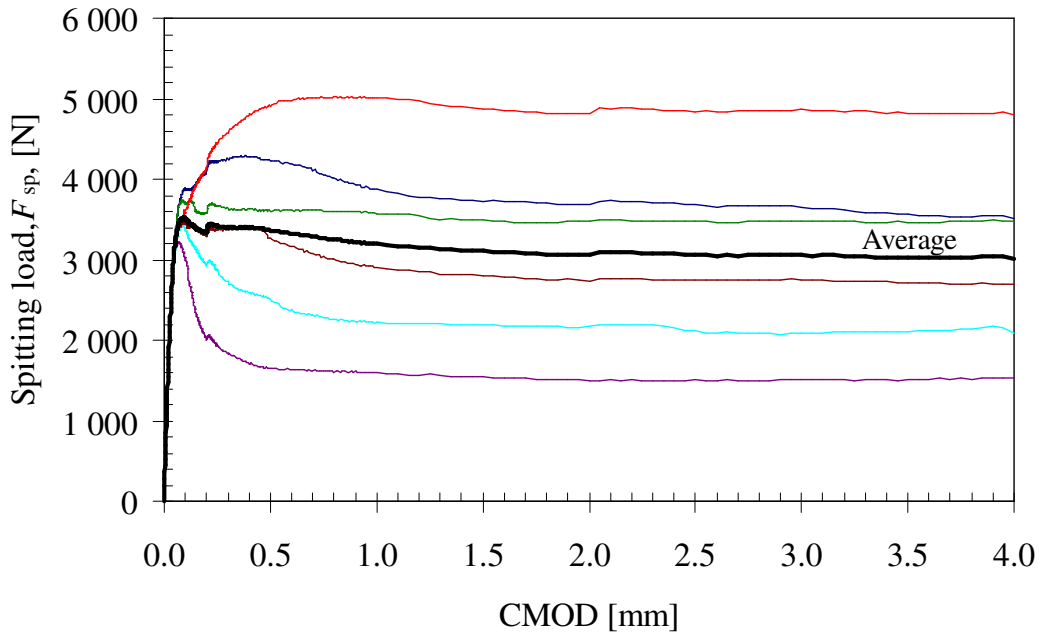

Figure 22. Splitting load-CMOD curve for the 200×200 mm² specimens tested at SP (Mix 2, 40 kg of 60 mm long fibres).

6 Comparison of test results

6.1 Comparison of splitting load-CMOD curves

The test results from each lab have been analysed and average splitting load-CMOD curves have been constructed. Furthermore, an average splitting load-CMOD curve based on the total test population (i.e. the individual test result from all labs) have also been calculated. The average curves for the 150×150 mm^2 specimens can be seen in Figure 23 while the average curves for the 200×200 mm^2 specimens can be seen in Figure 24. For the 150×150 mm^2 specimens, as can bee seen in Figure 23, there are only minor differences between the curves. For the 200×200 mm^2 specimens the differences seems to be larger, and mainly different levels of the post-peak load.

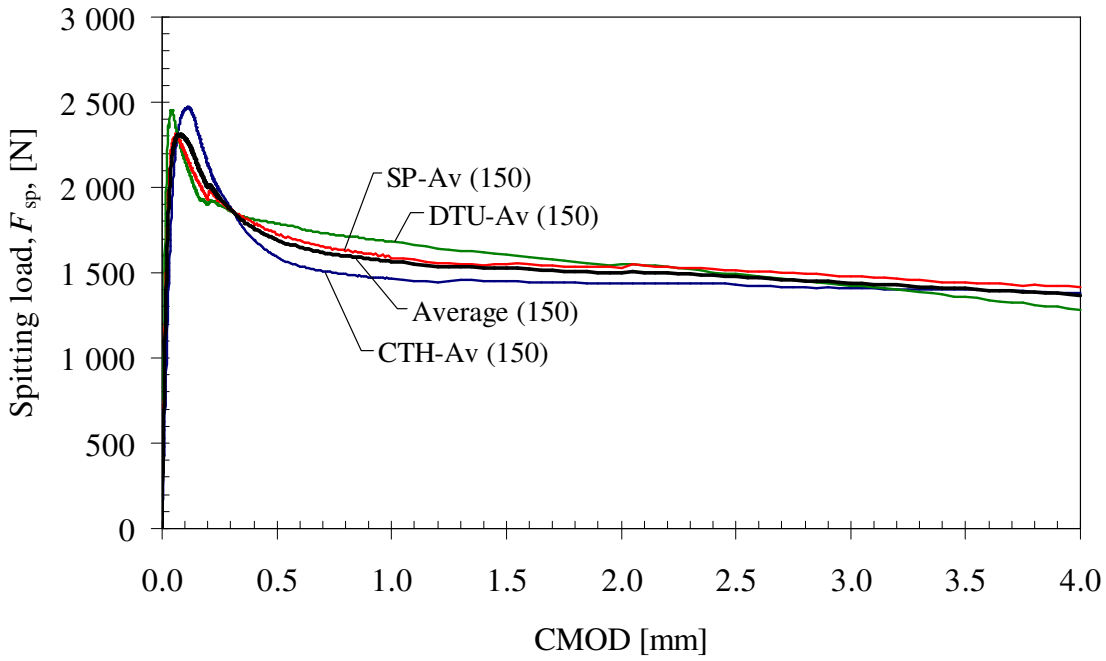

Figure 23. Splitting load versus CMOD for the 150×150 mm^2 specimens (Mix 1, 40 kg of 35 mm long fibres) - comparison of average values from each lab and total average.

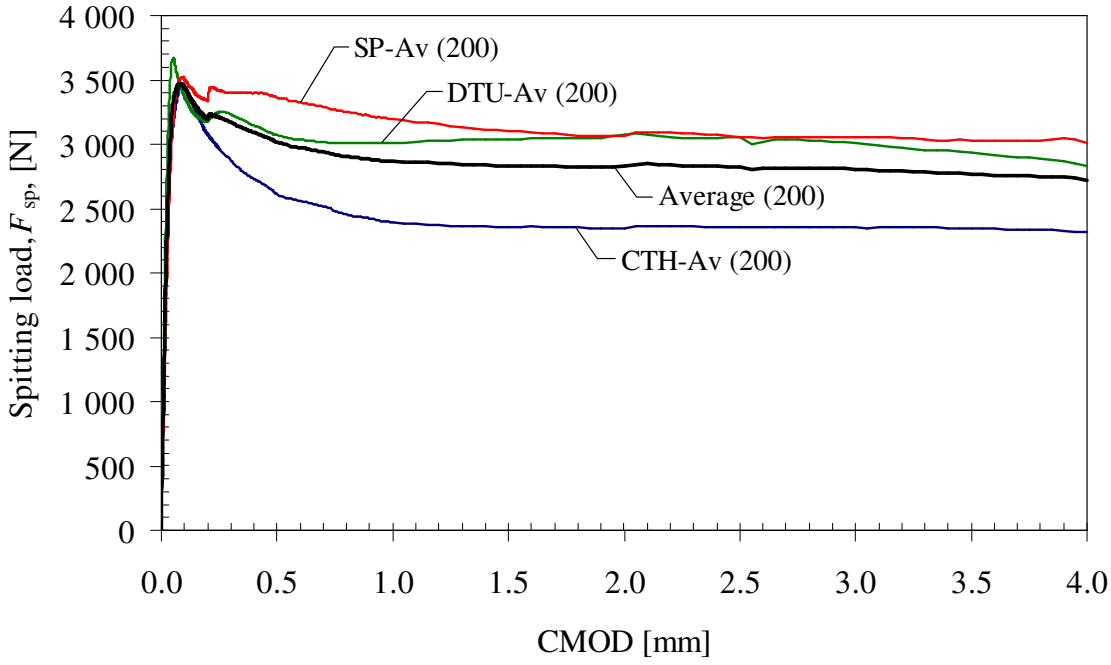

Figure 24. Splitting load versus CMOD for the 200×200 mm² specimens (Mix 2, 40 kg of 60 mm long fibres) - comparison of average values from each lab and total average.

6.2 Comparison of dissipated energy

By evaluating the specific energy dissipated during fracture, $G_{f.CMOD}$, at different *CMOD*s the scatter in the test results can be compared excluding the errors introduced when interpreting the test data by means of an inverse analysis. The work of fracture, W_f, can be calculated from the area under the splitting load-*CMOD* diagram. The specific energy dissipated, G_F, is the work of fracture, W_F, divided by the ligament area, A_{lig}, which is the projected area on a plane parallel to the ideal crack direction. However, in these tests the specimens are not completely fractured, i.e. there will always be a compression zone, which theoretically should be accounted for when calculating the ligament area. On the other hand, as it is difficult to determine the actual length of the fracture zone it has been assumed that the whole ligament height could be used. It should be pointed out that the evaluated fracture energy is not suitable as a material parameter for design. Furthermore, it is not possible to directly compare the dissipated energy between the two specimen sizes as the measured *CMOD* corresponds to different crack openings at the tip of the notch depending on the geometry of the specimen. On the other hand, the dissipated energy may be used as a qualitative indicator when comparing different FRC compositions.

Figure 25 shows the average dissipated energy for the 150×150 mm² specimens while Figure 26 shows the same for the 200×200 mm² specimens. Similar to the splitting load, the results for the 150×150 mm² specimens show good agreement while for the 200×200 mm² specimens the results from CTH seem to give lower values.

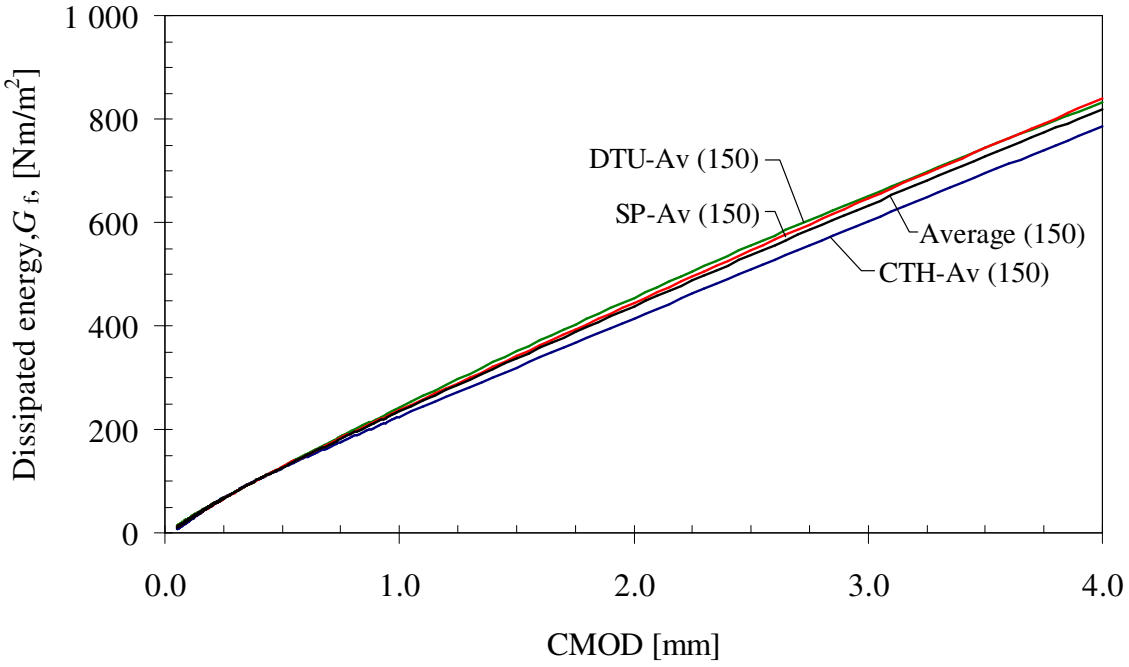

Figure 25. Dissipated energy versus CMOD for the 150×150 mm^2 specimens (Mix 1, 40 kg of 35 mm long fibres) - comparison of average values from each lab and total average.

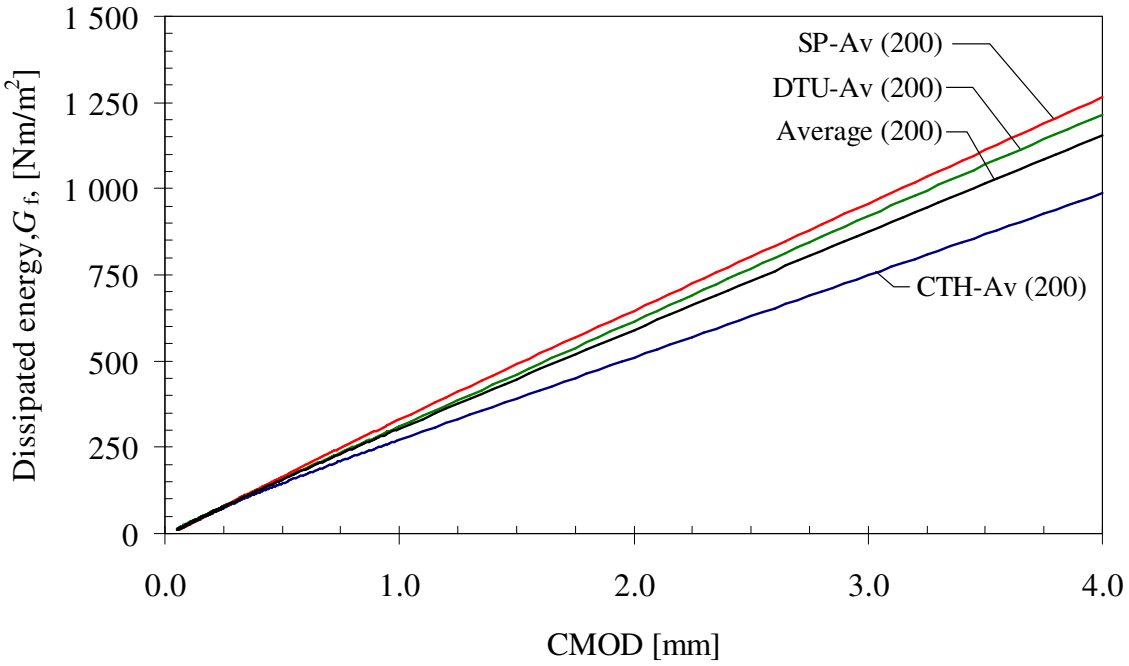

Figure 26. Dissipated energy versus CMOD for the 200×200 mm^2 specimens (Mix 2, 40 kg of 60 mm long fibres) - comparison of average values from each lab and total average.

6.3 Intra-lab variation

When testing steel-fibre reinforced concrete it is often found that the scatter is quite large, and the coefficient of variance (Cov) can be as high as 40%. In this study, the coefficient of variance for the splitting load has been calculated, both individually for each lab and for the total test population. In Figure 27 the coefficient of variance for the 150×150 mm^2 specimens can be seen and Figure 28 shows the same for the 200×200 mm^2 specimens. The scatter is quite large; for the 150×150 mm^2 specimens the average coefficient of variance is around 24% while it is 32% for the 200×200 mm^2 specimens. The reason for the scatter being larger for the 200×200 mm^2 specimens is believed to be related to the fibre dimensions. The longer fibres lead to a larger scatter since there are fewer fibres present. The coefficient of variance has also been calculated for the dissipated energy, see Figure 29 and Figure 30. For the dissipated energy the coefficient of variance is 20% for the 150×150 mm^2 specimens respectively 30% for the 200×200 mm^2 specimens.

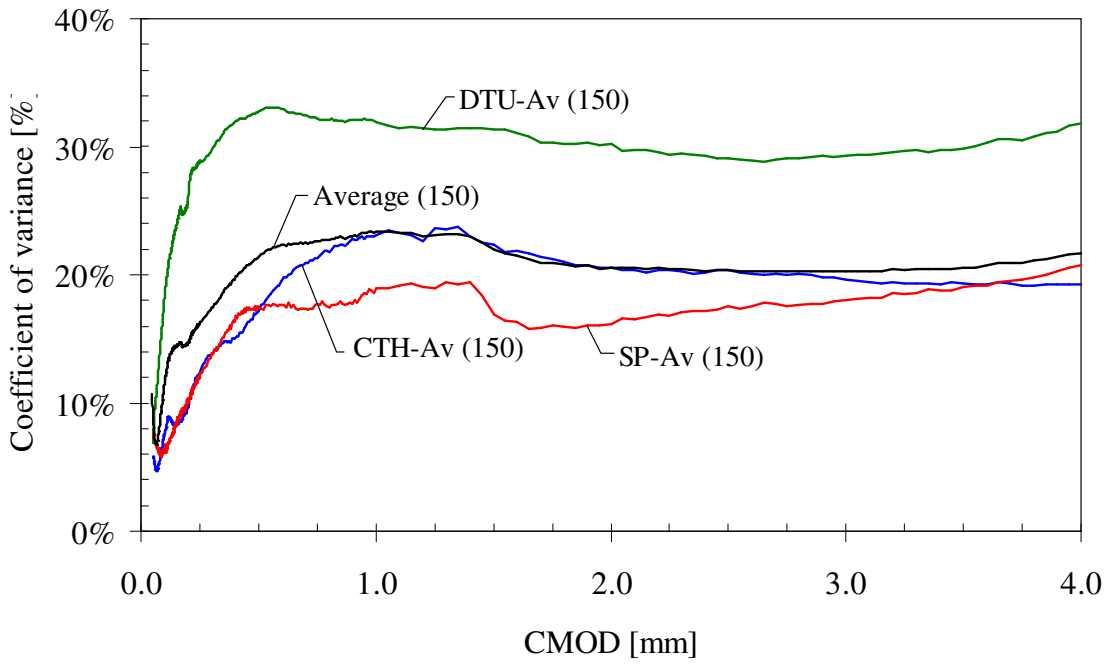

Figure 27. Coefficient of variance for the splitting load for the 150×150 mm^2 specimens (Mix 1, 40 kg of 35 mm long fibres) - comparison of values from each lab and total average.

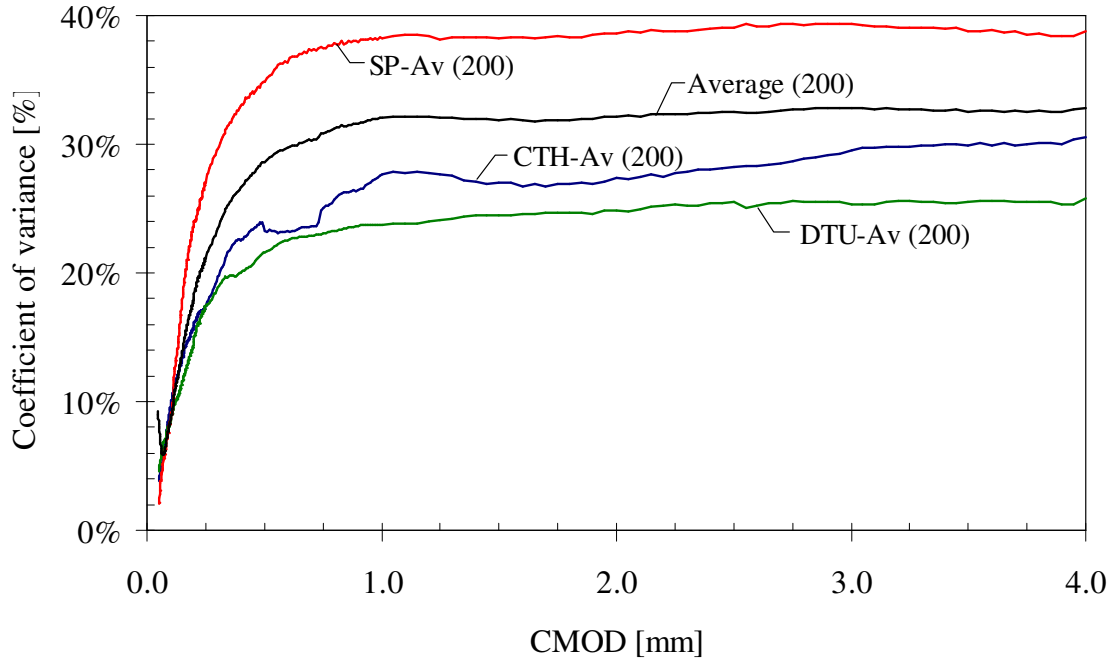

Figure 28. Coefficient of variance for the splitting load for the 200×200 mm² specimens (Mix 2, 40 kg of 60 mm long fibres) - comparison of values from each lab and total average.

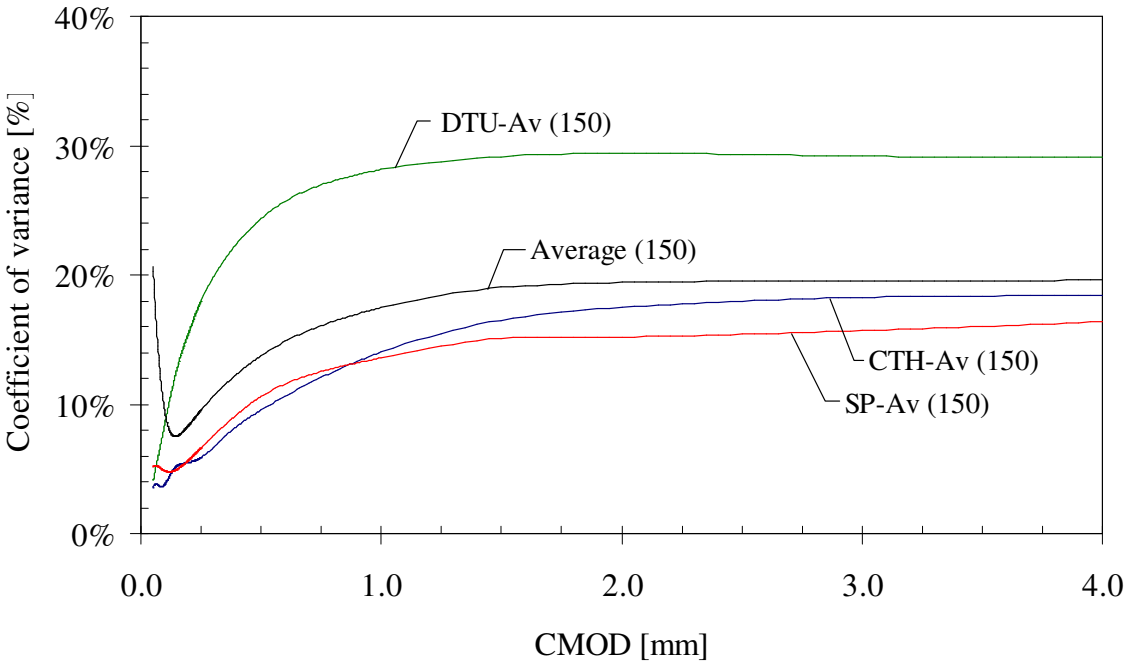

Figure 29. Coefficient of variance for the dissipated energy for the 150×150 mm² specimens (Mix 1, 40 kg of 35 mm long fibres) - comparison of values from each lab and total average.

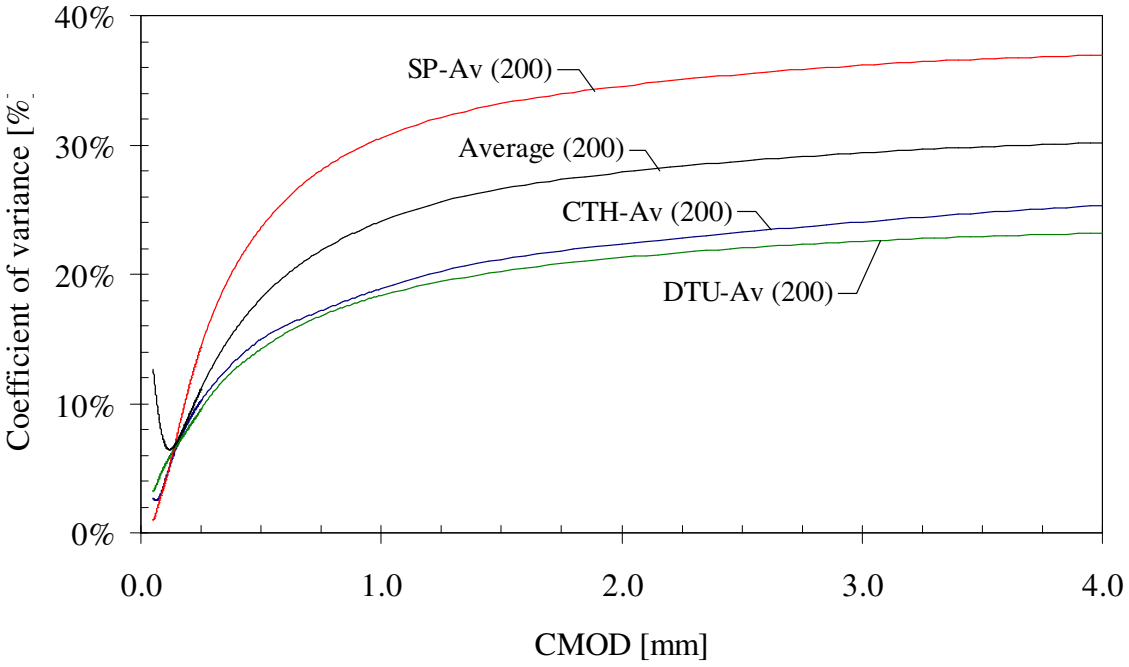

Figure 30. Coefficient of variance for the dissipated energy for the 200×200 mm^2 specimens (Mix 2, 40 kg of 60 mm long fibres) - comparison of values from each lab and total average.

6.4 Inter-lab variation

In this round robin test programme, tests were carried out at three labs. To evaluate the reproducibility of the test method, it is important to determine whether there are significant differences introduced by carrying out the test in different labs. A comprehensive study using statistical methods was carried out to investigate the level of variation obtained for the following parameters:

- the peak-load;
- the load at CMOD = 1.0 mm;
- the load at CMOD = 2.0 mm;
- the load at CMOD = 3.0 mm;
- the load at CMOD = 4.0 mm;
- the dissipated energy to a CMOD = 4.0 mm; and
- the number of fibres per square centimetre.

Thus, in this study, the analysis of variance method (more commonly known as ANOVA) is used. In essence, the ANOVA method is able to indicate whether there are any significant differences in the test results at a particular confidence level. After carrying out the analysis, a *p-value* will be computed. This *p-value* is an indication of the difference in the test results. The level of confidence is represented by the value of α. Normally, in statistical inferences, a value of $\alpha = 0.05$ is adopted. This value of α has been used in this study.

The ANOVA has four statistical parameters of interest:

- The $F_{statistic}$, which is the ratio of the Mean Squares (*MS*) for each source; which is the ratio (*SS* / *df*) of the Sum of Squares (*SS*) to the degrees of freedom (*df*) associated with each source.
- The *p-value*, which is derived from the calculated degrees of freedom of *F*. As *F* increases, the *p-value* decreases.
- The F_{critic}, which is derived from statistical tables based on the level of confidence, α, and the degrees of freedom associated with the test results.
- The ratio of the F_{static} and the F_{critic}. A value greater than unity would indicate that there is a significant difference between the treatments based on the level of confidence, α.

If the *p-value* is near zero, this casts doubt on the null hypothesis and suggests that at least one sample-mean is significantly different from the other sample-means. The choice of a critical *p-value* to determine whether the result is judged "statistically significant" is left to the researcher. It is common to declare a result significant if the *p-value* is less than 0.05 or 0.01.

The following tables (Table 12 to Table 17) show the measured parameters and the results of the ANOVA can be seen in Table 18 and Table 19. The ANOVA shows that for all the considered parameters (for both the 150×150 mm^2 and the 200×200 mm^2 specimens) there is no significant difference between the treatments other than the internal variation – in all analyses the ratio of F_{stat}/F_{crit} is less than unity. Hence, there is no inter-lab variation and the test result can be said to be independent of the testing location and the equipment used (with *CMOD*-control or without).

Table 12. Comparison of peak loads (F_{max}).

WST 150 F_{max}				**WST 200 F_{max}**			
Spec	CTH	DTU	SP	Spec	CTH	DTU	SP
1	2538		2321	1	3825	3724	(4290)*
2	2466	2464	2431	2	3471	3837	3744
3	2518	2633	2286	3	3891	3909	(5024) *
4	2846	2472	2575	4	3037	3723	3446
5	2194	2323	2107	5	3526	3487	3221
6	2356		2282	6	3440	3897	3470
Average:	2486	2473	2334	Average:	3532	3763	3470
Cov [%]:	8.65%	5.12%	6.75%	Cov [%]:	8.66%	4.19%	6.17%
Total average:		2426		Total average:		3603	
Total Cov [%]:		7.45%		Total Cov [%]:		7.12%	

* Values has been omitted from ANOVA as the specimens contained more fibres and the peak-value occurred for a much larger *CMOD* than for the other specimens.

Table 13. Comparison of the load at CMOD = 1.0 mm ($F_{1.0}$).

	WST 150 $F_{1.0}$				**WST 200 $F_{1.0}$**		
Spec	CTH	DTU	SP	Spec	CTH	DTU	SP
1	1515		1036	1	2711	2738	3882
2	1221	1106	1797	2	1435	3766	3573
3	1454	2307	1851	3	3440	3424	5008
4	2077	1926	1767	4	2250	2161	2224
5	1434	1390	1521	5	2361	2266	1601
6	1094		1551	6	2153	3695	2903
Average:	1466	1682	1587	Average:	2392	3008	3198
Cov [%]:	22.02%	31.94%	19.00%	Cov [%]:	27.16%	24.92%	37.53%
Total average:		1565		Total average:		2866	
Total Cov [%]:		23.40%		Total Cov [%]:		32.07%	

Table 14. Comparison of the load at CMOD = 2.0 mm ($F_{2.0}$).

	WST 150 $F_{2.0}$				**WST 200 $F_{2.0}$**		
Spec	CTH	DTU	SP	Spec	CTH	DTU	SP
1	1473		1145	1	2579	2772	3695
2	1257	1001	1737	2	1424	3823	3470
3	1434	2014	1796	3	3394	3490	4823
4	1978	1849	1646	4	2239	2183	2175
5	1393	1326	1380	5	2270	2287	1501
6	1106		1452	6	2154	3897	2735
Average:	1440	1547	1526	Average:	2344	3075	3066
Cov [%]:	19.64%	30.21%	16.15%	Cov [%]:	26.93%	26.23%	37.77%
Total average:		1499		Total average:		2828	
Total Cov [%]:		20.61%		Total Cov [%]:		32.19%	

Table 15. Comparison of the load at CMOD = 3.0 mm ($F_{3.0}$).

	WST 150 $F_{3.0}$				**WST 200 $F_{3.0}$**		
Spec	CTH	DTU	SP	Spec	CTH	DTU	SP
1	1397		1079	1	2478	2785	3657
2	1246	941	1677	2	1391	3678	3474
3	1437	1774	1806	3	3546	3439	4862
4	1916	1773	1599	4	2300	2111	2094
5	1345	1214	1312	5	2189	2177	1506
6	1105		1391	6	2224	3860	2752
Average:	1408	1426	1477	Average:	2355	3008	3057
Cov [%]:	18.81%	29.25%	18.06%	Cov [%]:	29.16%	26.86%	38.53%
Total average:		1438		Total average:		2807	
Total Cov [%]:		20.26%		Total Cov [%]:		32.77%	

Table 16. Comparison of the load at CMOD = 4.0 mm ($F_{4.0}$).

WST 150 $F_{4.0}$				WST 200 $F_{4.0}$			
Spec	CTH	DTU	SP	Spec	CTH	DTU	SP
1	1348		974	1	2376	2482	3509
2	1244	835	1623	2	1361	3335	3470
3	1425	1587	1794	3	3545	3323	4803
4	1880	1663	1516	4	2315	2030	2089
5	1277	1035	1250	5	2062	2068	1525
6	1110		1317	6	2234	3732	2687
Average:	1381	1280	1412	Average:	2316	2828	3014
Cov [%]:	18.56%	31.83%	20.73%	Cov [%]:	30.30%	27.52%	37.96%
Total average:		1367		Total average:		2719	
Total Cov [%]:		21.73%		Total Cov [%]:		32.83%	

Table 17. Comparison of the dissipated energy to CMOD = 4.0 mm ($G_{f4.0}$).

WST 150 $G_{f4.0}$				WST 200 $G_{f4.0}$			
Spec	CTH	DTU	SP	Spec	CTH	DTU	SP
1	803		611	1	1069	1128	1504
2	706	566	924	2	659	1502	1421
3	794	1088	999	3	1417	1387	1961
4	1044	979	914	4	930	874	907
5	756	694	790	5	933	916	643
6	612		796	6	907	1481	1157
Average:	786	832	839	Average:	986	1215	1265
Cov [%]:	17.64%	29.16%	16.39%	Cov [%]:	24.92%	24.22%	36.32%
Total average:		817		Total average:		1155	
Total Cov [%]:		19.61%		Total Cov [%]:		30.17%	

Table 18. Compilation of ANOVA results for the 150×150 mm^2 specimens (Mix 1, 40 kg of 35 mm long fibres).

ANOVA analysis results for the 150×150 mm^2 specimens (Mix 1, 40 kg of 35 mm long fibres)						
	Considered parameter					
Statistical parameters	F_{max}	$F_{1.0}$	$F_{2.0}$	$F_{3.0}$	$F_{4.0}$	$G_{f4.0}$
F_{stat}	1.3015	0.4001	0.1610	0.0796	0.2221	0.1654
p-value	0.3053	0.6782	0.8530	0.9239	0.8038	0.8494
F_{crit}	3.8056	3.8056	3.8056	3.8056	3.8056	3.8056
F_{stat}/F_{crit}	0.342	0.105	0.042	0.021	0.058	0.043

Table 19. Compilation of ANOVA results for the 200×200 mm^2 specimens (Mix 2, 40 kg of 60 mm long fibres).

ANOVA analysis results for the 200×200 mm^2 specimens (Mix 2, 40 kg of 60 mm long fibres)						
	Considered parameter					
Statistical parameters	F_{max}	$F_{1.0}$	$F_{2.0}$	$F_{3.0}$	$F_{4.0}$	$G_{f4.0}$
F_{stat}	2.2513	1.3092	1.3258	1.1054	0.9818	1.1083
p-value	0.1447	0.2992	0.2950	0.3566	0.3974	0.3557
F_{crit}	3.8056	3.6823	3.6823	3.6823	3.6823	3.6823
F_{stat}/F_{crit}	0.592	0.356	0.360	0.300	0.267	0.301

6.5 Comparison of specimens fibre distribution

As the variation in the test results is quite large it was decided to determine and compare the fibre distribution. In all the tested specimens the total number of fibres were counted and the average number of fibres per square centimetre have been compared in Figure 31 and Figure 32. Furthermore, the coefficient of variance for the number of fibres per square centimetre can be seen in Figure 33. From the figures it becomes clear that the scatter in the fibre distribution is quite large, for the short fibre (35 mm) the coefficient of variance varies between 6% and 18% while for the long fibre (60 mm) it varies between 28% and 38%. However, ANOVA analyses of the fibre distribution, see Table 20 and Table 21, indicate no difference between the specimens tested at the labs.

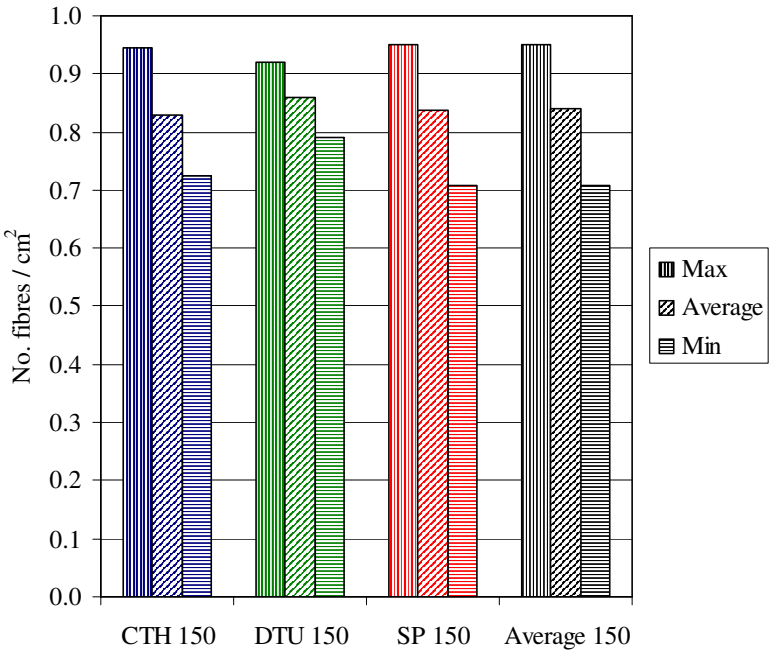

Figure 31. Comparison of the number of fibres per square centimetre for the 150×150 mm^2 specimens (Mix 1, 40 kg of 35 mm long fibres) – max, average, and min.

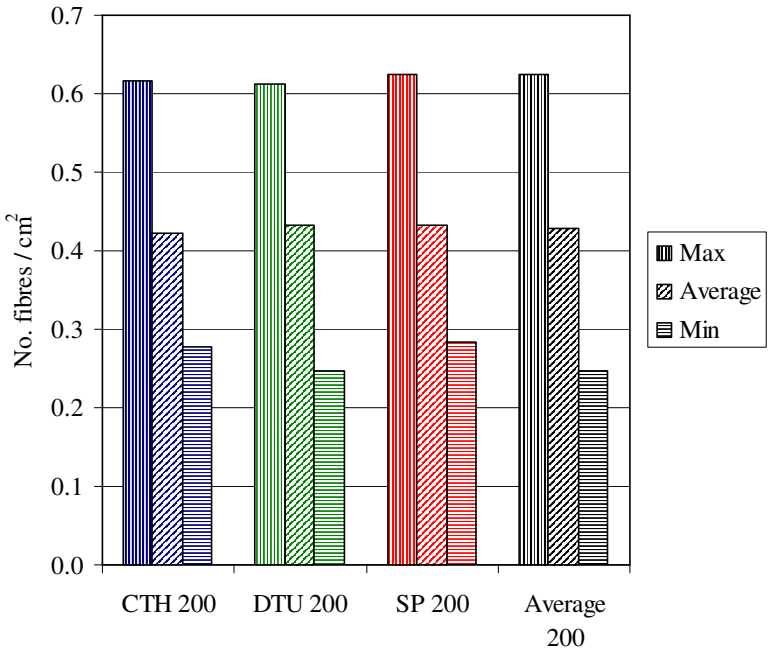

Figure 32. Comparison of the number of fibres per square centimetre for the 200×200 mm^2 specimens (Mix 2, 40 kg of 60 mm long fibres) – max, average, and min.

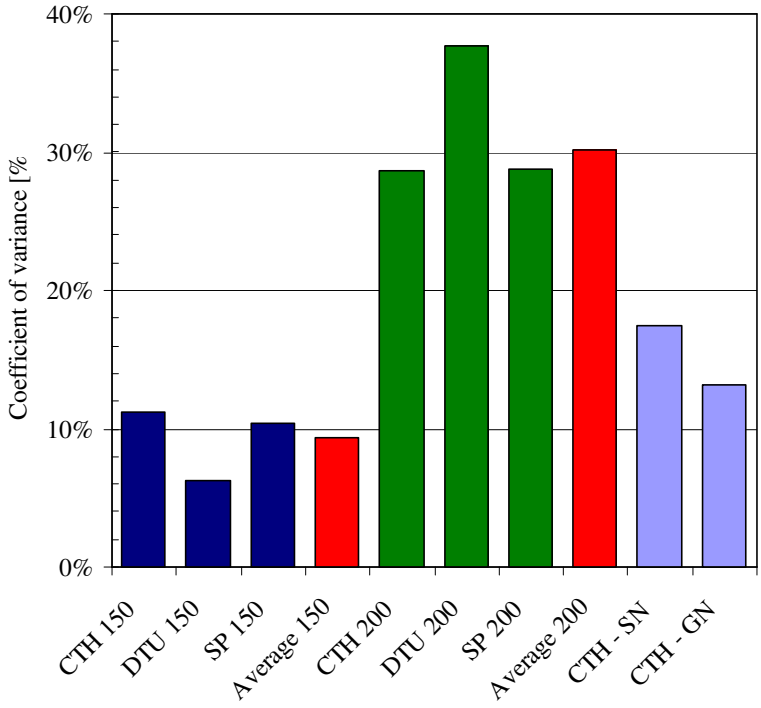

Figure 33 Coefficient of variance for number of fibres per square centimetre (no. fibres / cm^2).

Table 20. Comparison of fibre distribution for the 150×150 mm^2 specimens (Mix 1, 40 kg of 35 mm long fibres) and for the 200×200 mm^2 specimens (Mix 2, 40 kg of 60 mm long fibres).

WST 150 ***No. fibres / cm^2***				**WST 200** ***No. fibres / cm^2***			
Spec	CTH	DTU	SP	Spec	CTH	DTU	SP
1	0.725		0.708	1	0.62	0.349	0.461
2	0.835	0.853	0.787	2	0.28	0.539	0.498
3	0.824	0.880	0.951	3	0.49	0.613	0.625
4	0.945	0.919	0.831	4	0.32	0.248	0.283
5	0.724	0.790	0.833	5	0.40	0.271	0.322
6	0.919		0.915	6	0.42	0.580	0.405
Average:	0.829	0.861	0.837	Average:	0.421	0.433	0.432
Cov [%]:	11.51%	6.30%	10.46%	Cov [%]:	28.68%	40.40%	28.46%
Total average:	0.840			Total average:	0.429		
Total Cov [%]:	9.38%			Total Cov [%]:	30.14%		

Table 21. ANOVA results for the fibre distribution for the 150×150 mm^2 specimens (Mix 1, 40 kg of 35 mm long fibres) and for the 200×200 mm^2 specimens (Mix 2, 40 kg of 60 mm long fibres).

Statistical parameters	150×150 mm^2 specimens (Mix 1, 40 kg 35 mm long fibres)	200×200 mm^2 specimens (Mix 2, 40 kg 60 mm long fibres)
F_{stat}	0.181	0.0137
p-value	0.836	0.9864
F_{crit}	3.806	3.6823
F_{stat}/F_{crit}	0.048	0.0037

7 The effect of the guide notch

The average splitting load-CMOD curves can be seen in Figure 34 and the coefficient of variance for the splitting load can be seen in Figure 35. From the test results it seems as if the splitting load for the specimens with the guide notch is slightly higher, both the peak load and the post peak load. Furthermore, as can be seen in Figure 35, the scatter seems to be lower for the specimens with the guide notch. The dissipated energy, which can be seen in Figure 36, is higher for the specimens with a guide notch (but the scatter is lower, see Figure 37); on average the ratio between the dissipated energies for specimens with a guide notch in relation to specimens without is 1.25. However, as can be seen in Figure 38 there appears to be more fibres present in the specimens with the guide notch. The reason for this is unclear, but it is clear that it has a large influence on the measured load and the dissipated energy and for this reason it is difficult to draw any specific conclusions. However, as can be seen in Figure 39, which shows a specimen without a guide notch with two visible cracks, there are some problems with the cracking in the specimens without a guide notch.

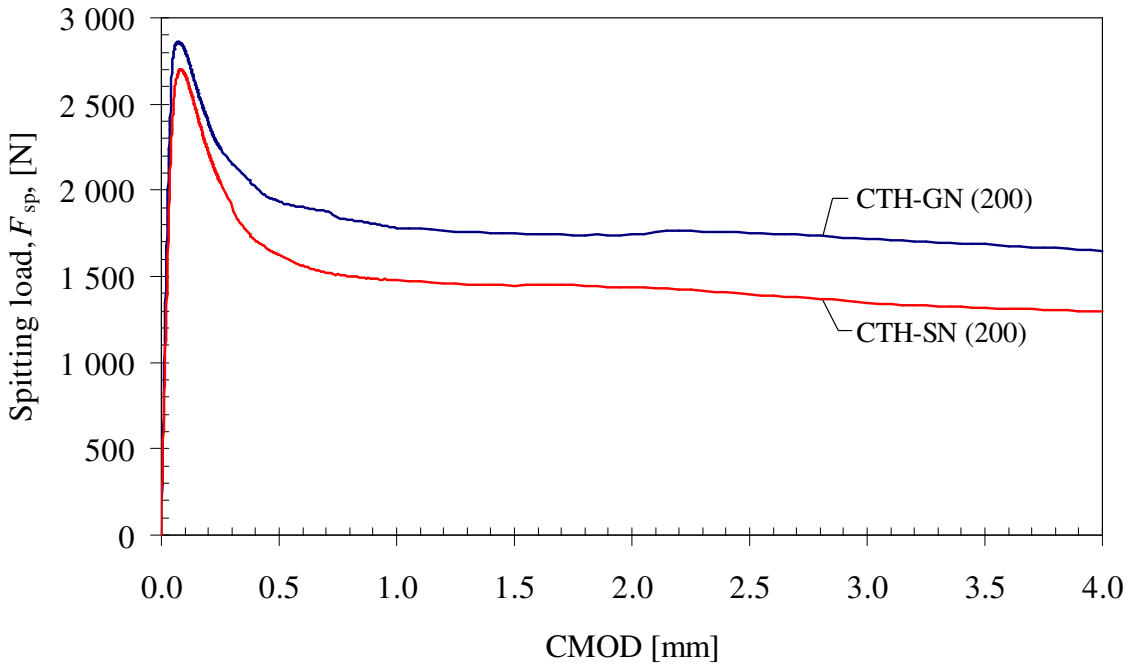

Figure 34. Comparison of average splitting load versus CMOD for the 200×200 mm^2 specimens with and without a guide notch (Mix 1, 40 kg of 35 mm long fibres) – GN = with guide notch.

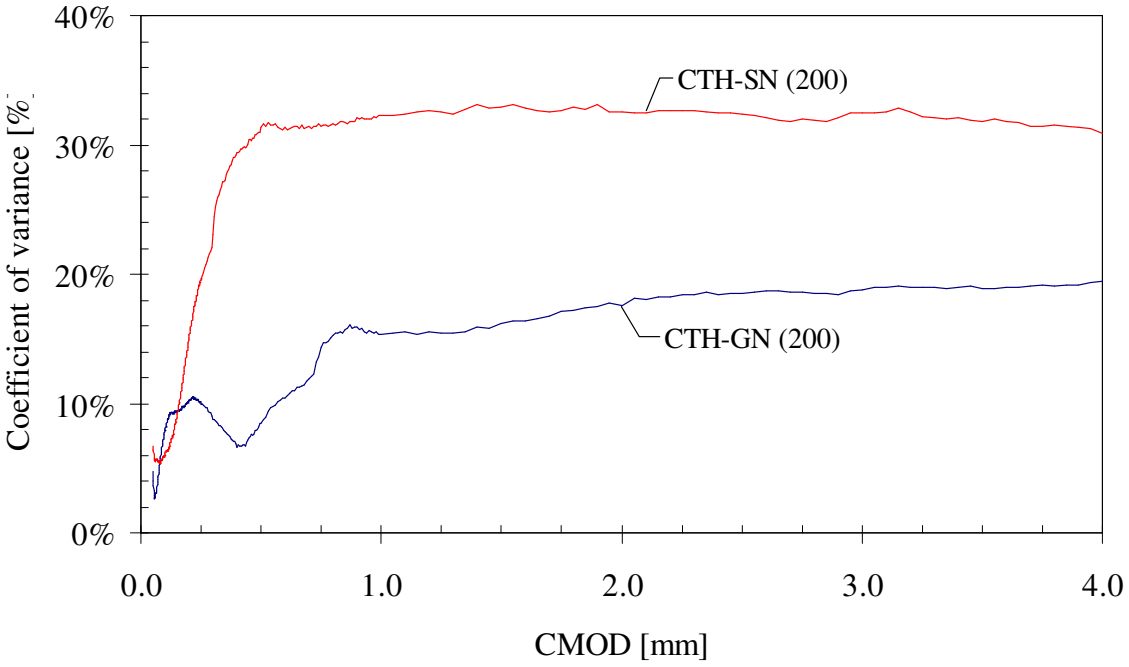

Figure 35. Coefficient of variance for the splitting load for the 200×200 mm^2 specimens with and without a guide notch (Mix 1, 40 kg of 35 mm long fibres) - GN = with guide notch.

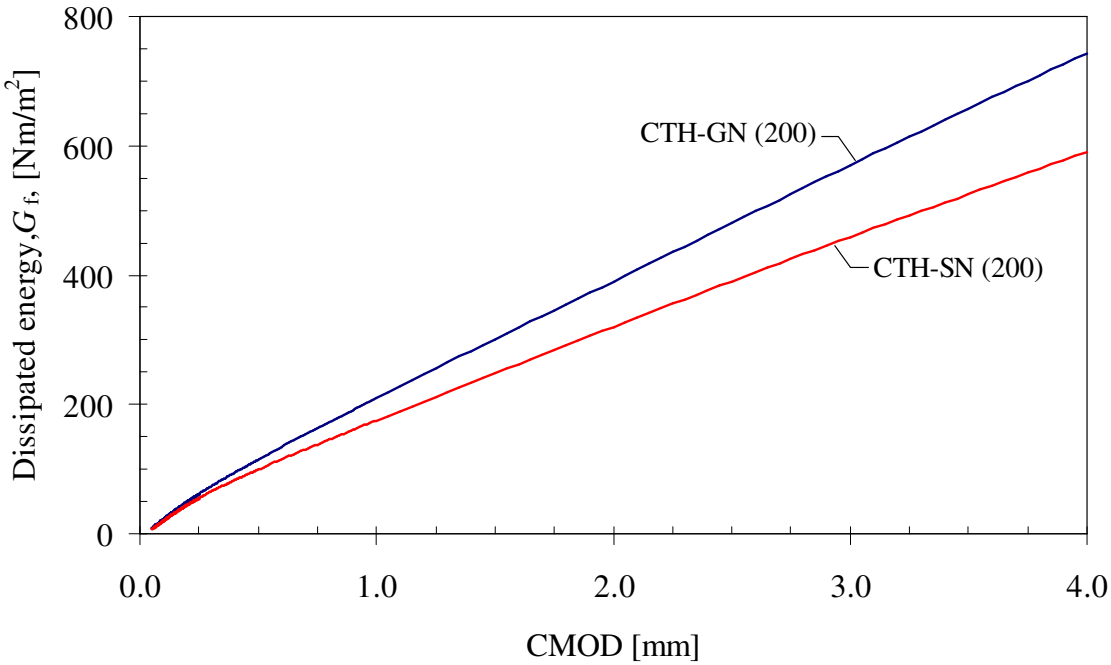

Figure 36. Dissipated energy versus CMOD for the 200×200 mm^2 specimens with and without a guide notch (Mix 1, 40 kg of 35 mm long fibres) - GN = with guide notch.

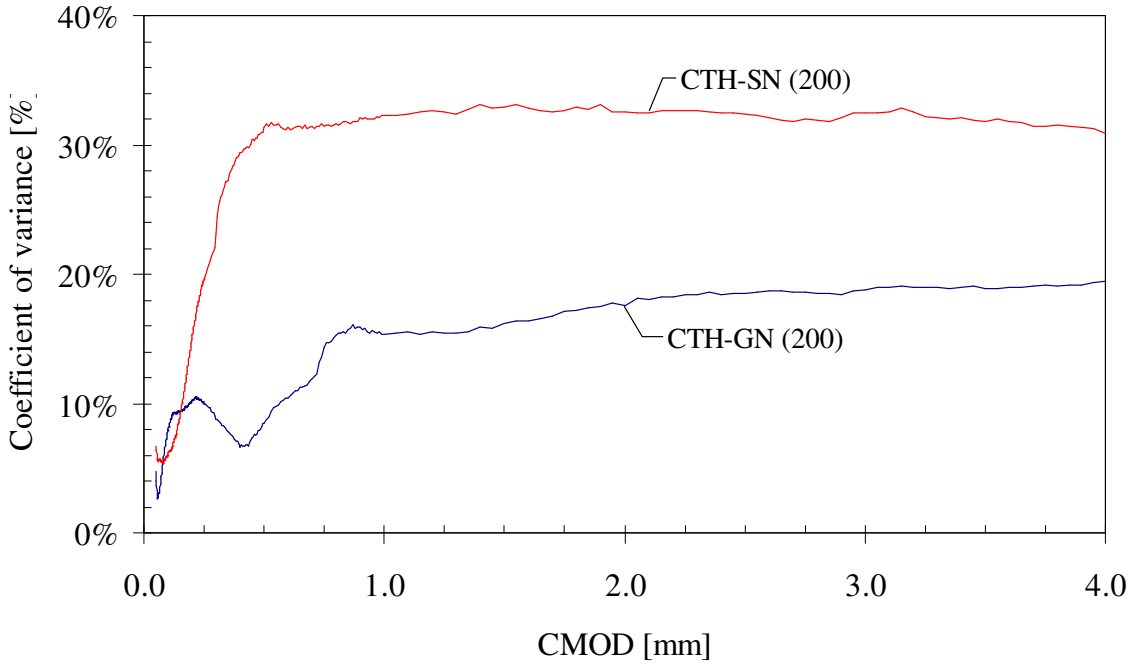

Figure 37. Coefficient of variance for the dissipated energy for the 200×200 mm^2 specimens with and without a guide notch (Mix 1, 40 kg of 35 mm long fibres) - GN = with guide notch.

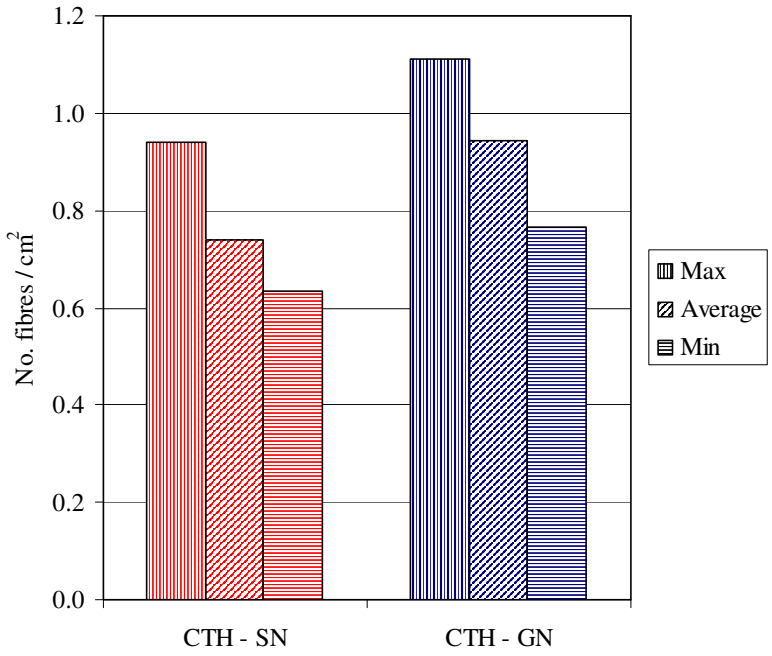

Figure 38. Comparison of the number of fibres per square centimetre for the 200×200 mm^2 specimens with and without a guide notch (40 kg of 35 mm long fibres) – GN = with guide notch (Mix 1, 40 kg of 60 mm long fibres) – max, average, and min.

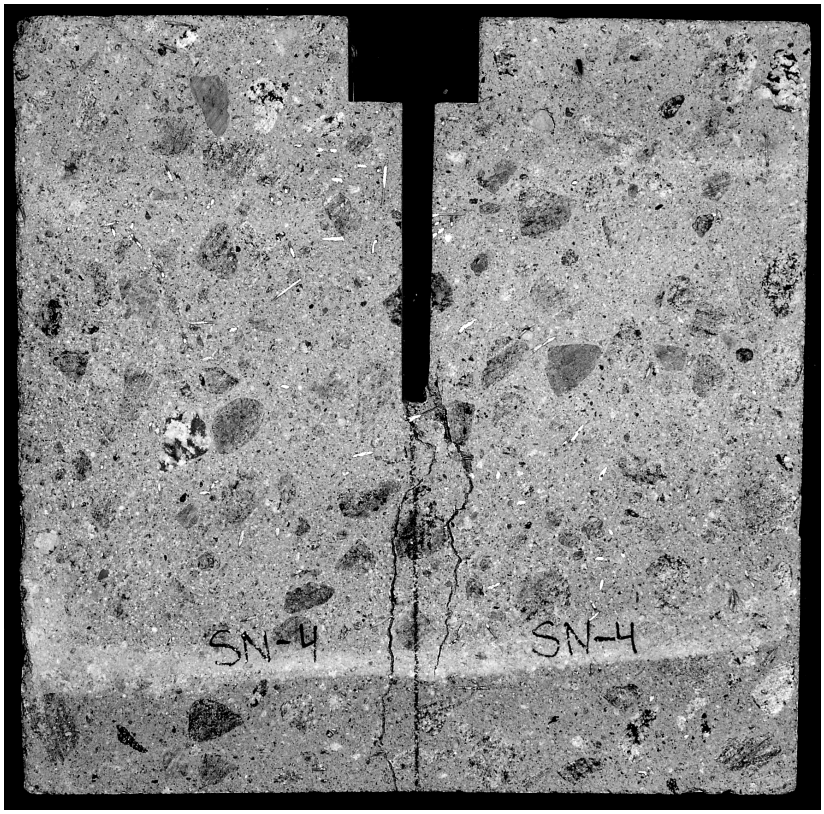

Figure 39. Specimen without guide notch with two cracks.

8 Interpretation of test results

8.1 Results from inverse analysis

As the main benefit from fibre reinforcement is the ability to transfer stress across a crack it is important to characterise the stress-crack opening relationship. The stress-crack opening relationship is also required for advanced (non-linear) analysis of structural behaviour (cracking, crack propagation, and fracture). Hence, to show how the test results may be interpreted, inverse analyses were conducted on the averaged load-*CMOD* curves (the average of all tested specimens from one mix). The inverse analysis was conducted using a Matlab® program, developed at DTU by Østergaard (2003), which is based on the cracked hinge model by Olesen (2001), see Østergaard & Olesen (2004), which uses the fictitious crack concept by Hillerborg et al. (1976), see also Hillerborg (1980). In the cracked hinge model it was assumed that the σ-w relationship could be approximated by a bi-linear function, see Figure 40.

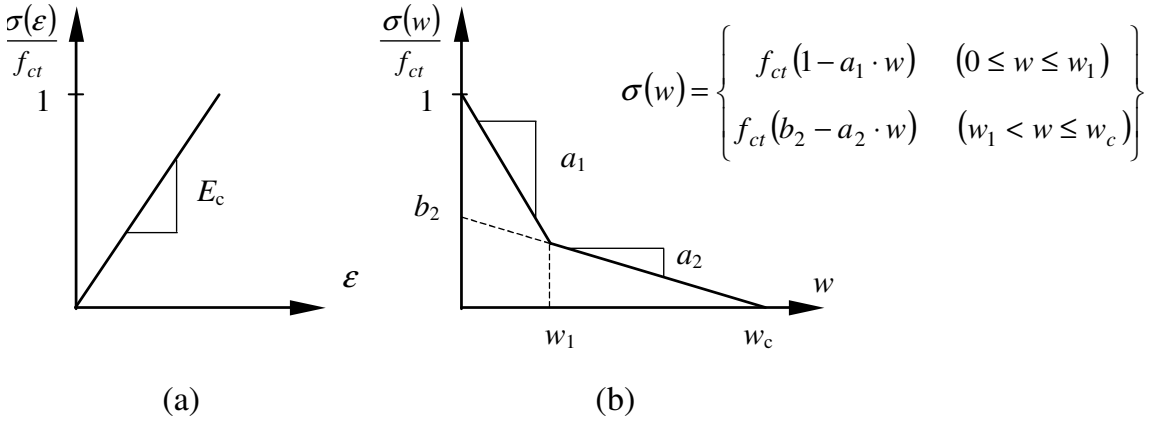

Figure 40. Assumed bi-linear stress-crack opening relationship and definition of the parameters describing the relationship.

In Table 22 the result of the inverse analyses can be seen. The bi-linear stress-crack opening relationships for the 150×150 mm^2 (Mix 1, 40 kg of 35 mm long fibres) specimens can be seen in Figure 41 and in Figure 42 for the 200×200 mm^2 specimens (Mix 2, 40 kg of 60 mm long fibres). There are some minor differences between the obtained stress-crack opening relationships but the overall agreement is quite good. The biggest differences are found in the post-cracking parameters (a_1, a_2, and b_2), which is expected as these are highly influenced by the fibre orientation and distribution.

Table 22. Results of the inverse analyses on the test results: for the 150×150 mm² specimens (Mix 1, 40 kg of 35 mm long fibres) the 200×200 mm² specimens (Mix 2, 40 kg of 60 mm long fibres).

	WST 150						WST 200					
	f_{ct}	a_1	a_2	b_2	%error		f_{ct}	a_1	a_2	b_2	%error
	[MPa]	[mm^{-1}]	[mm^{-1}]	[-]			[MPa]	[mm^{-1}]	[mm^{-1}]	[-]	
CTH	2.05	10.01	0.0463	0.399	2.38	CTH	2.18	10.0	0.055	0.48	3.20
DTU	1.98	15.12	0.1187	0.508	2.36	DTU	2.49	22.1	0.041	0.51	2.34
SP	1.90	10.256	0.0748	0.490	2.58	SP	2.46	20.0	0.026	0.54	2.61
Average:	1.98	11.80	0.080	0.47	2.44	Average:	2.37	17.4	0.040	0.51	2.71
Cov:	3.9%			12.5%		Cov:	7.2%			5.7%	

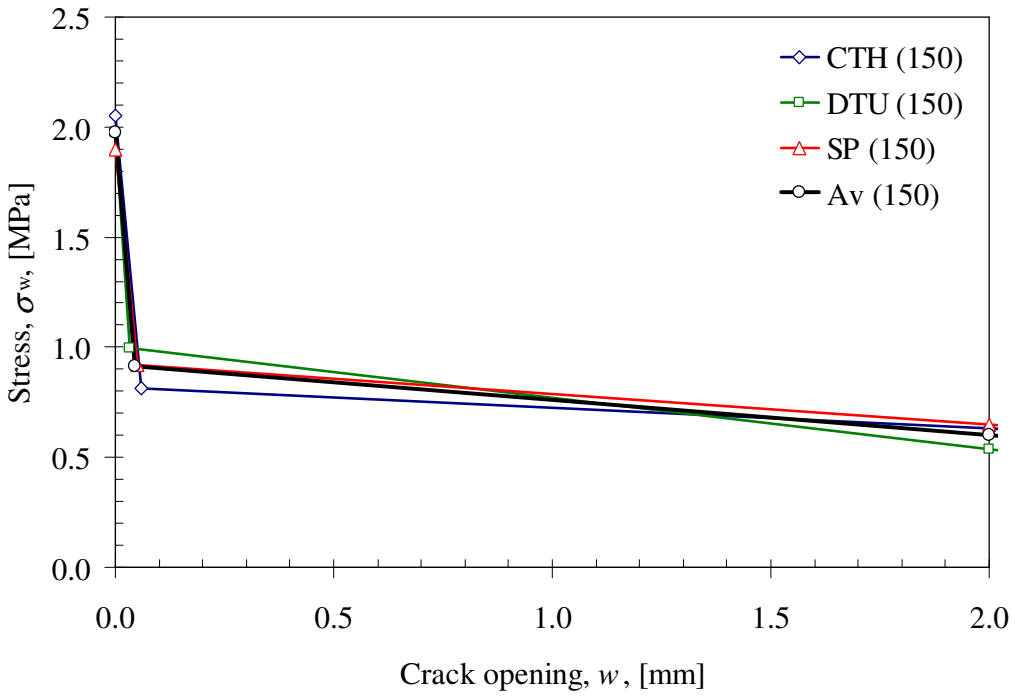

Figure 41. Comparison of stress-crack opening relationships (σ-w) obtained by inverse analysis for the 150×150 mm² specimens (Mix 1, 40 kg of 35 mm long fibres).

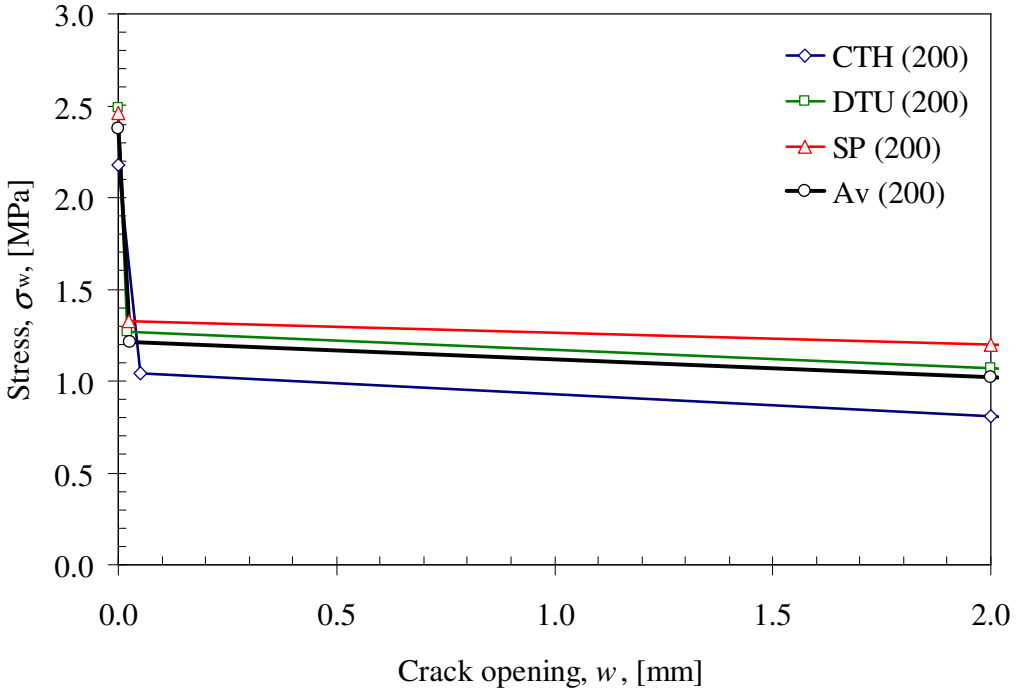

Figure 42. Comparison of stress-crack opening relationships (σ-w) obtained by inverse analysis for the 200×200 mm2 specimens (Mix 2, 40 kg of 60 mm long fibres).

Table 23. Results of the inverse analyses on the test results of the 200×200 mm^2 specimens with and without a guide notch (Mix 1, 40 kg of 35 mm long fibres) - GN = with guide notch.

WST 200 SN & GN					
	f_{ct}	a_1	a_2	b_2	%error
	[MPa]	[mm^{-1}]	[mm^{-1}]	[-]	
CTH-SN	1.74	10.00	0.0626	0.368	2.92
CTH-GN	1.87	10.00	0.0542	0.424	2.34

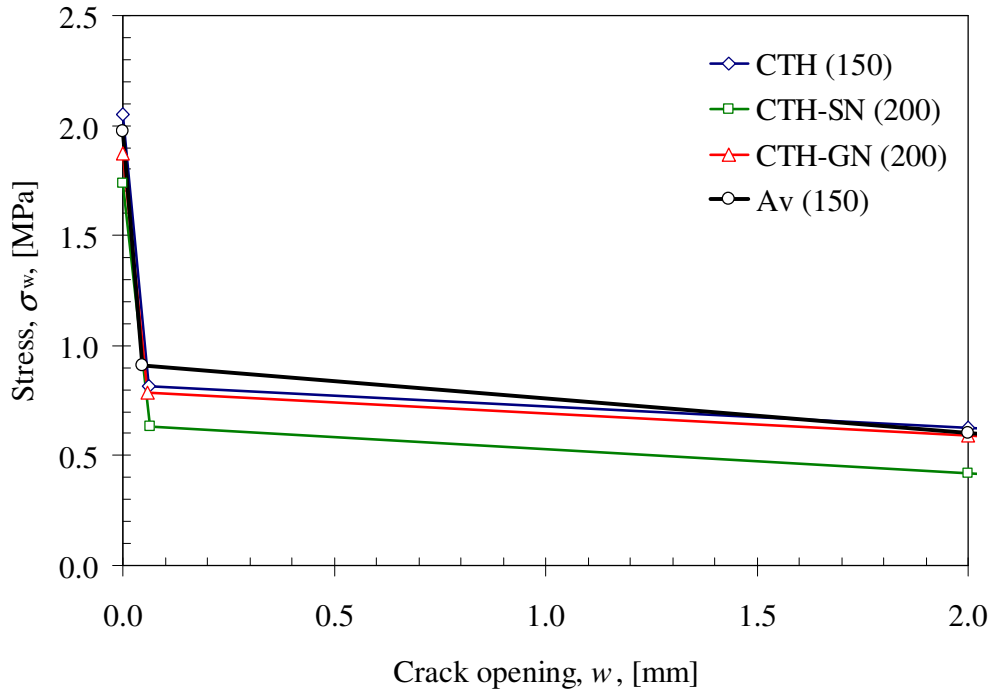

Figure 43. Comparison of stress-crack opening relationships (σ-w) obtained by inverse analysis for the 200×200 mm^2 specimens with and without a guide notch - GN = with guide notch - and the 150×150 mm^2 specimens (all from Mix 1, 40 kg of 35 mm long fibres).

8.2 Results from simplified analysis

A residual tensile stress, f_{tR}, can be determined by the simplified approach described in section 3. The relationships between *CMOD* and *CTOD* (eqv. 2 & 3) can be used to calculate the corresponding crack opening, w.

For the 150×150 mm^2 WST-specimens, the relationship between the *CMOD* and the *CTOD* is given by eqv. 2. This leads to a crack opening, w, for the maximum *CMOD* which is:

$$CTOD = 0.551 \cdot CMOD - 0.0084$$
$$\Rightarrow w = 0.551 \cdot 4.0 - 0.0084$$
$$w = 2.20 \ \ mm$$

For the 200×200 mm^2 WST-specimens, the relationship between the *CMOD* and the *CTOD* is given by eqv. 3. This leads to a crack opening, w, for the maximum *CMOD* which is:

$$CTOD = 0.533 \cdot CMOD - 0.0110$$
$$\Rightarrow w = 0.533 \cdot 4.0 - 0.0110$$
$$w = 2.12 \ \ mm$$

Figure 44 show the external forces acting on the specimen and the internal forces, based on the simplified stress distribution. The residual tensile stress, f_{tR} can be calculated by

solving the equilibrium equation of forces (eqv. 6) and the equilibrium equation of moment with respect to the position of the neutral axis (eqv. 7):

$$F_{tR} - F_c - F_{sp} = 0 \qquad \text{(eqv. 6)}$$

$$F_{tR} \cdot \left(\frac{h^* - x}{2} \right) + F_c \cdot \left(\frac{2}{3} x \right) - F_{sp} \left(d_y - x - \frac{(CMOD/2)^2}{d_y - x} \right) - \frac{F_v}{2} \left(\frac{d_x + CMOD}{2} \right) = 0 \qquad \text{(eqv. 7)}$$

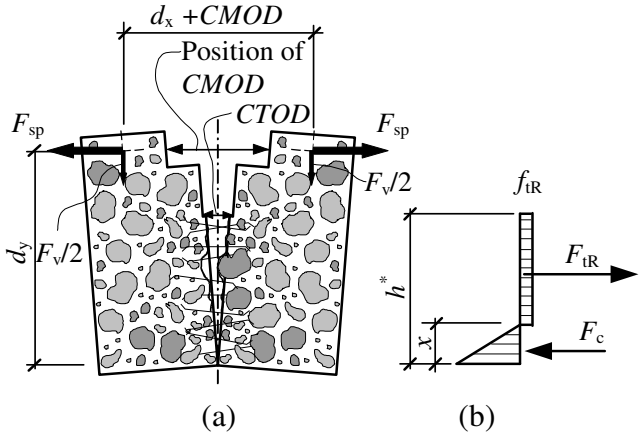

Figure 44. (a) Schematic view of a cracked specimen and the definition of CMOD and CTOD. (b) Simplified stress distribution based on the assumption of a constant residual tensile stress f_{tR} (x denotes the height of the compressive zone).

As an example the residual tensile stress, f_{tR}, for the 150×150 mm^2 specimens tested at CTH can be calculated with the following data:

- the average splitting load F_{sp}, at CMOD = 4.0 mm is 1381 N;
- the distance, d_y, from the bottom of the specimen to the point where the splitting load is applied is 135 mm;
- the distance, d_x, between the loading points is 80 mm;
- the length, h^*, of the ligament is 76.65 mm; and
- the width, l, of the ligament is 99.2 mm.

This gives:

$$F_v = \frac{F_{sp}}{1.866} = \frac{1381}{1.866} = 740 \ [N]$$

$$x = \frac{h^*}{10} = \frac{76.65}{10} = 7.67 \ [mm]$$

$$F_c = F_{tR} - F_{sp} = F_{tR} - 1381 \ [N]$$

$$F_{tR} \cdot \left(\frac{76.65 - 7.67}{2} \right) + (F_{tR} - 1381) \cdot \left(\frac{2}{3} 6.67 \right) - 1381 \left(135 - 7.67 - \frac{(4.0/2)^2}{135 - 7.67} \right) - \frac{740}{2} \left(\frac{80 + 4.0}{2} \right) = 0$$

$$\Rightarrow F_{tR} = 5009.9 \ \ [N]$$

$$\Rightarrow f_{tR} = \frac{F_{tR}}{\left(h^* - x\right)\cdot l} = \frac{5009.9}{(76.65 - 7.67)\cdot 99.2} = 0.73 \ \ [MPa]$$

The result of the simplified analysis can be seen in Table 24 and in Figure 45 to Figure 47 where the residual tensile stress, f_{tR}, is compared with the bi-linear stress-crack opening relationship determined by inverse analysis. As can be seen, the residual tensile stress, f_{tR}, is an average value of the bi-linear stress-crack opening relationship.

Table 24. Results of the simplified analyses to determine the residual stress f_{tR}: for the 150×150 mm² specimens (Mix 1, 40 kg of 35 mm long fibres), the 200×200 mm² specimens (Mix 2, 40 kg of 60 mm long fibres), and the 200×200 mm² specimens with and without a guide notch (Mix 1, 40 kg of 35 mm long fibres).

	WST 150 f_{tR}	**WST 200** f_{tR}	**WST 200-SN** f_{tR}	**WST 200-GN** f_{tR}
	[MPa]	[MPa]	[MPa]	[MPa]
CTH	0.73	0.97	0.53	0.71
DTU	0.70	1.19	-	-
SP	0.77	1.27	-	-

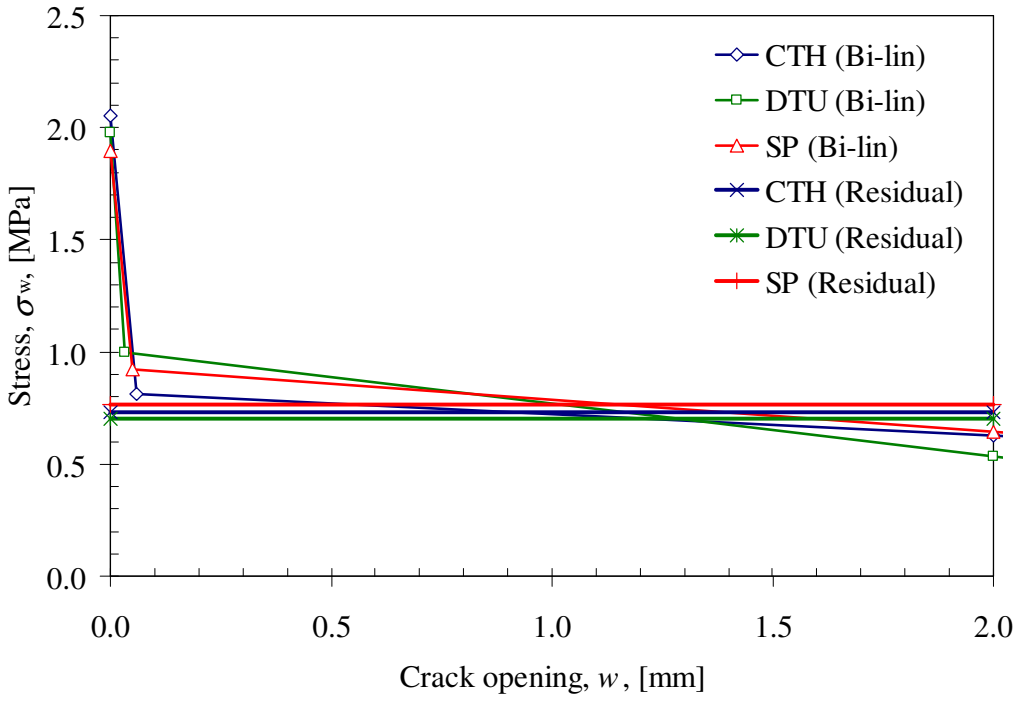

Figure 45. Comparison between the simplified analysis (the residual tensile stress f_{tR}) and the inverse analysis for the 150×150 mm² specimens (Mix 1, 40 kg of 35 mm long fibres).

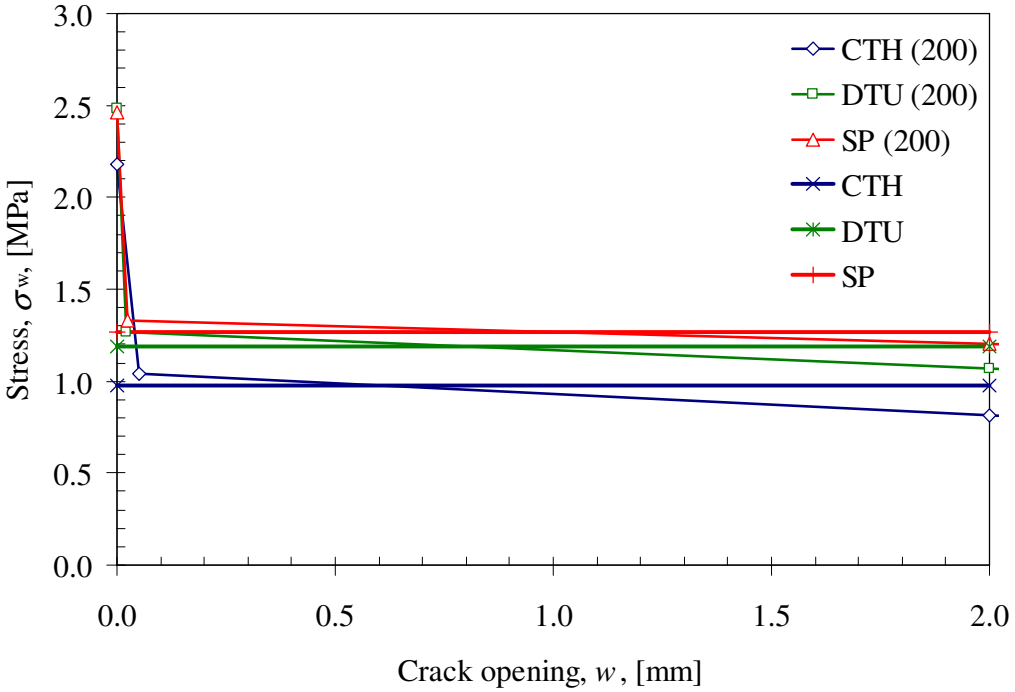

Figure 46. Comparison between the simplified analysis (the residual tensile stress f_{tR}) and the inverse analysis for the 200×200 mm^2 specimens (Mix 2, 40 kg of 60 mm long fibres).

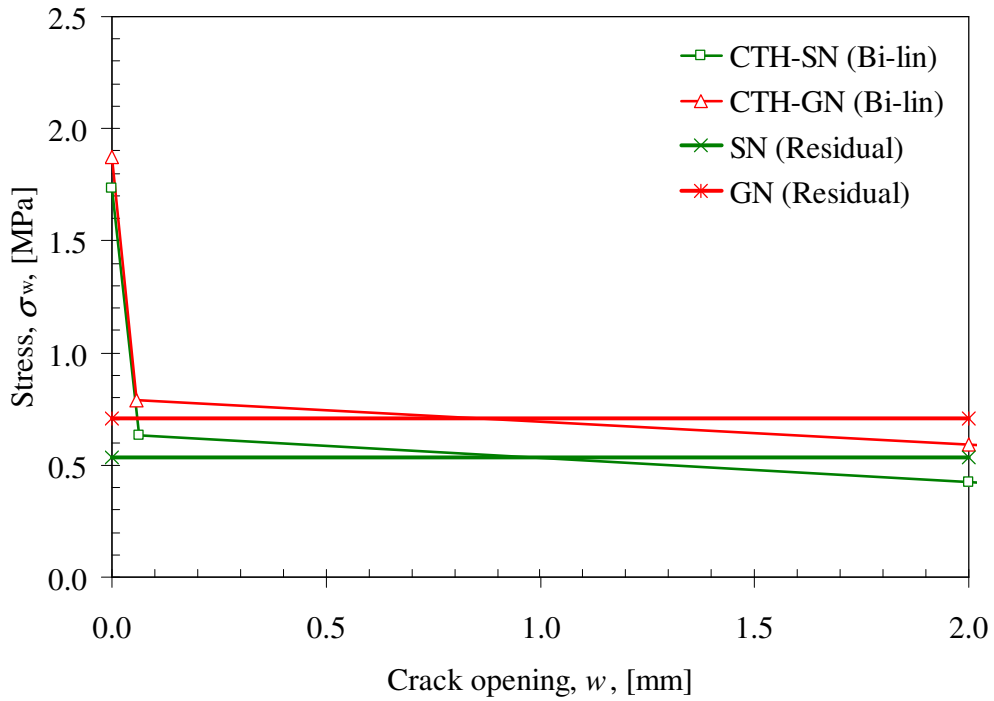

Figure 47. Comparison between the simplified analysis (the residual tensile stress f_{tR}) and the inverse analysis for the 200×200 mm^2 specimens with and without a guide notch - GN = with guide notch (Mix 1, 40 kg of 35 mm long fibres).

9 Concluding remarks

To evaluate the reproducibility of the wedge-splitting test method, a round robin study was conducted in which three labs participated. The participating labs were:

- DTU – Technical University of Denmark, Department of Civil Engineering;
- CTH – Chalmers University of Technology, Department of Structural Engineering and Mechanics; and
- SP – Swedish National Testing and Research Institute.

Two different mixes were investigated; the difference between the mixes was the fibre length (Mix 1 with 40 kg of 35 mm long fibres and Mix 2 with 40 kg of 60 mm long fibres). The test results from each lab were analysed and a study of the variation was performed. From the study of the intra-lab variations, it is evident that the variations of the steel fibre-reinforced concrete properties are significant. The coefficient of variance for the splitting load was found to vary between 20 to 35% for the 150×150 mm^2 specimens (Mix 1, 40 kg of 35 mm long fibres) while for the 200×200 mm^2 specimens (Mix 2, 40 kg of 60 mm long fibres) it varied between 25 to 40%. The investigation of the inter-lab variation, based on an analysis of variance (ANOVA) indicated that there is no inter-lab variation. The test result can be said to be independent of the testing location and the equipment used (with or without *CMOD*-control).

The conclusions that can be drawn from this study are that:

- the wedge-splitting test method is a suitable test method for assessment of fracture properties of steel fibre-reinforced concrete;
- the test method is easy to handle and relatively fast to execute
- the test result was found to be independent of the testing location and the equipment used;
- the test can be run with CMOD-control or without, in a machine with a constant cross-head displacement rate (if rate is equal to or less than 0.25 mm/min);
- due to variations in fibre distribution, the scatter of the test results is high (but not higher than for the three-point bending test);
- the dimensions of the specimen (height, width, and thickness) should, if possible, be four times the maximum fibre length, or at least more than three times the fibre length;
- using inverse analysis, the tensile fracture properties can be interpreted from the test result as a bi-linear stress-crack opening relationship.

10 References

ACI Committee 544: 'Measurement of properties of fiber reinforced concrete'. *ACI Materials Journal* 85(1988), pp. 583-593.

ASTM C 1018: '*Standard Test Method for Flexural Toughness and First-Crack Strength of Fiber-Reinforced Concrete (Using Beam With Third-Point Loading),*' ASTM, West Conshohocken, Pa., 1997.

ASTM C 1550: '*Standard Test Method for Flexural Toughness of Fiber-Reinforced Concrete (Using Centrally-Loaded Round Panel)*,' ASTM, West Conshohocken, Pa., 2002.

Barr B., Gettu R., Al-Oraimi S.K.A., and Bryars L.S. (1996): 'Toughness measurement – the need to think again'. *Cem. & Concrete Composites* 18(1996), pp. 281-297.

Bolzon G., Fedele R., and Maier G. (2002): 'Parameter identification of a cohesive crack model by Kalman filter', *Comput. Methods Appl. Mech. Engrg*. 191(2002), pp. 2847-2871.

Brühwiler, E. and Wittmann, F.H. (1990): 'The wedge splitting test, a new method of performing stable fracture mechanics test' *Eng. Fracture Mech*. 35(1/2/3), 117-125.

de Place Hansen, E.J., Hansen, E.A., Hassanzadeh, M., and Stang, H. (1998): Determination of the Fracture Energy of Concrete: A comparison of the Three-Point Bend Test on Notched Beam and the Wedge-Splitting Test. NORDTEST Project No 1327-97. SP Swedish National Testing and Research Institute, Building Technology, SP Report 1998:09, Borås, Sweden. p. 87.

Elser M., Tschegg E.K., Finger N., and Stanzl-Tschegg S.E. (1996): 'Fracture Behaviour of Polypropylene-Fibre reinforced Concrete: an experimental investigation', *Comp. Science and Technology*, 56(1996), pp. 933-945.

Gapalaratnam V.S. and Gettu R. (1995): 'On the characterization of flexural toughness in fiber reinforced concretes'. *Cem. & Concrete Composites* 17(1995), pp. 239-254.

Hillerborg, A., Modeer, M., and Petersson, P.E. (1976): 'Analysis of Crack Formation and Crack Growth in Concrete by Means of Fracture Mechanics and Finite Elements'. *Cem. & Concrete Res.* 6, 1976, 773-782.

Hillerborg, A. (1980): 'Analysis of Fracture by Means of the Fictitious Crack Model, Particularly for Fibre Reinforced Concrete'. *The Int. J. Cem. Comp.* 1980. 2. 177-184.

Kim J.-K. and Kim Y.-Y. (1999): 'Fatigue crack growth of high-strength concrete in wedge-splitting test'. *Cem. and Concrete Research*, 29(1999), pp. 705–712.

Kitsutaka Y. (1997): 'Fracture parameters by polylinear tension-softening analysis. *J. of Eng. Mechanics*, 123(5) pp. 444-450, 1997.

Kooiman, A.G. (2000): '*Modelling Steel Fibre Reinforced Concrete for Structural Design*'. Ph.D. Thesis, TU Delft 2000.

Leite J.P. de B., Slowik V. and Mihashi H. (2004): *'Mesolevel models for simulation of fracture behaviour of fibre reinforced concrete'*. In Fibre-Reinforced Concrete, Proceedings of the Sixth International RILEM Symposium, ed. di Prisco et al. 2004.

Linsbauer, H.N. and Tschegg, E.K. (1986) 'Fracture energy determination of concrete with cube shaped specimens', *Zement und Beton*, 31, pp 38-40.

Löfgren I (2004). *'The wedge splitting test – a test method for assessment of fracture parameters of FRC?'*. In Fracture Mechanics of Concrete Structures, Li Et al (eds), 2004.

Löfgren I, Stang H, and Olesen JF (2004): *'Wedge splitting test – a test to determine fracture properties of FRC'* BEFIB 2004 - Sixth RILEM symposium on fibre reinforced concrete (FRC): Varenna, Italy, 20th-22nd September 2004.

Meda A., Plizzari G.A., and Slowik V. (2001): *'Fracture of fiber reinforced concrete slabs on grade'*. In Fracture Mechanics of Concrete Structures, ed. De Borst et al, 2001.

Nanakorn P. and Horii H. (1996): 'Back analysis of tension-softening relationship of concrete. *J. Materials, Conc. Struct.*, Pavements, 32(544), pp. 265-275, 1996.

Nemegeer D., Vanbrabant J. and Stang H. (2003): 'Brite Euram Program on Steel Fibre Concrete Subtask: Durability: *Corrosion Resistance of Cracked Fibre Reinforced Concrete'*. In Test and Design Methods for Steel Fibre Reinforced Concrete – Background and Experiences - Proceedings of the RILEM TC 162-TDF Workshop, Ed Schnütgen and Vandevalle, 2003.

NORDTEST (1999): 'NT BUILD 491- Concrete and Mortar, Hardened: Fracture Energy (mode I) - Three-Point Bend Test on Notched Beams'. Approved 1999-11, Espoo Finland.

Olesen, J.F. (2001) 'Fictitious crack propagation in fibre-reinforced concrete beams'. *Journal of Eng. Mech*. 127(3): pp. 272-280, 2001.

Olesen, J.F., Østergaard, L. and Stang, H. (2003): "Fracture Mechanics and Plasticity Modelling of the Split Cylinder Test", Proc. Int. Symp. "Brittle Matrix Composites 7", A.M. Brandt et al. (eds.), October 13-15, 2003, ZTUREK RSI and Woodhead Publ., Warsaw, pp. 467-476.

Planas J., Guinea G.V., and Elices M. (1999): 'Size effect and inverse analysis in concrete fracture', *International Journal of Fracture*, 95(1999), pp. 367-378.

Que, N.S. and Tin-Loi, F. (2002): 'Numerical evaluation of cohesive fracture parameters from a wedge splitting test' *Engineering Fracture Mechanics*, 69 (2002), pp. 1269-1286.

RILEM TC-50 FMC (1985): 'Determination of the fracture energy of mortar and concrete by means of three-point bend tests on notched beams', *Materials and Structures*, 18(106), 1985, pp. 285.

RILEM Report 5 (1991): *Fracture Mechanics Test Methods for Concrete*. Edited by S.P. Shah and A. Carpinteri. Chapman and Hall, London, 1991.

RILEM TC TDF-162 (2000): 'σ–ε Design Method' *Materials and Structures*, 33 March 2000, pp. 75-81.

RILEM TC TDF-162 (2001): 'Test and design methods for steel fibre reinforced concrete. Recommendations for uni-axial tension test', *Materials and Structures*, 34 Jan-Feb 2001, pp. 3-6.

RILEM TC TDF-162 (2002a): 'Test and design methods for steel fibre reinforced concrete. Bending test – Final Recommendation', *Materials and Structures*, 35, Nov 2002, pp. 579-582.

RILEM TC TDF-162 (2002b): 'Design of steel fibre reinforced concrete using the σ–w method – principles and applications' *Materials and Structures*, 35 June 2002, pp. 262-278.

Roelfstra P.E. and Wittmann F.H. (1986): 'Numerical method to link strain softening with failure of concrete. In *Fracture Toughness and Fracture Energy of Concrete*, pp. 163-175. Elsevier, 1986.

Romualdi J.P. and Mandel J.A. (1964): 'Tensile strength of concrete affected by uniformly distributed and closely spaced short lengths of wire reinforcement'. *ACI J. Proc*. 61(6) 1964, pp. 657-671.

Sousa, J.L.A.O, Gettu, R., and Barragán, B.E. (2002): 'Obtaining the σ–w curve from the inverse analysis of the notched beam response' see Annex D of Barragán, B.E. (2002) '*Failure and toughness of steel fiber reinforced concrete under tension and shear*', Ph.D. Thesis, Universitat Politécnica de Catalunya, Barcelona, Spain, 2002.

Trunk, B., Schober, G., and Wittmann, F.H. (1999): 'Fracture mechanics parameters of autoclaved aerated concrete', *Cem. and Concrete Research*, 29(1999), pp. 855-859.

Uchida, Y., Kurihara, N., Rokugo, K., and Koyanagi, W. (1995): 'Determination of tension softening diagrams of various kinds of concrete by means of numerical analysis'. In *Fracture Mechanics of Concrete Structures*, FRAMCOS-2, ed. F.H. Wittmann, pp. 17-30, 1995.

Østergaard, L. (2003) '*Early-Age Fracture Mechanics and Cracking of Concrete – Experiments and Modelling'*. Ph.D thesis, Department of Civil Engineering, Technical University of Denmark. 2003.

Østergaard & Olesen (2004): 'Comparative study of fracture mechanical test methods for concrete'. In *Fracture Mechanics of Concrete Structures*, FRAMCOS-5, ed. Li et al, pp. 455-462.

Østergaard, L., Olesen, J.F., Stang, H., and Lange, D. (2002): *On the interpretation of the wedge splitting test by application of the cracked hinge model*. DTU, Denmark, Course material; Behavior and Performance of Early Age Concrete, 2002.

Que, N.S. and Tin-Loi, F. (2002): Numerical evaluation of cohesive fracture parameters from a wedge splitting test. *Engineering Fracture Mechanics*, 69 (2002), pp. 1269-1286.

Appendix A – ANOVA

The ANOVA table has eight columns:

- The first shows the source of the variability.
- The second shows the Sum of Squares (*SS*) due to each source.
- The third shows the degrees of freedom (*df*) associated with each source.
- The fourth shows the Mean Squares (*MS*) for each source, which is the ratio *SS* / *df*.
- The fifth shows the $F_{statistic}$, which is the ratio of the *MS's*.
- The sixth shows the *p-value*, which is derived from the cdf of *F*. As *F* increases, the *p-value* decreases.
- The seventh shows the F_{critic}, which is derived from statistical tables based on the level of confidence, α, and the degrees of freedom associated with the test results.
- The eight shows the ratio of the F_{static} and the F_{critic}. A value greater than unity would indicate that there is a significant difference between the treatments based on the level of confidence, α.

If the *p-value* is near zero, this casts doubt on the null hypothesis and suggests that at least one sample mean is significantly different than the other sample means. The choice of a critical *p-value* to determine whether the result is judged "statistically significant" is left to the researcher. It is common to declare a result significant if the *p-value* is less than 0.05 or 0.01.

Table 25. ANOVA results for the maximum load for the 150×150 mm² specimens (Mix 1, 40 kg of 35 mm long fibres).

Source of Variation	*SS*	*df*	*MS*	F_{stat}	*p-value*	F_{crit}	F_{stat}/F_{crit}
Between Groups	81786	2	40893	1.3015	0.3053	3.8056	0.342
Within Groups	408468	13	31421				
Total	490253	15					

Table 26. ANOVA results for the load at CMOD = 1.0 mm for the 150×150 mm² specimens (Mix 1, 40 kg of 35 mm long fibres).

Source of Variation	*SS*	*df*	*MS*	F_{stat}	*p-value*	F_{crit}	F_{stat}/F_{crit}
Between Groups	116713	2	58356	0.4001	0.6782	3.8056	0.105
Within Groups	1896223	13	145863				
Total	2012936	15					

Table 27. ANOVA results for the load at CMOD = 2.0 mm for the 150×150 mm² specimens (Mix 1, 40 kg of 35 mm long fibres).

Source of Variation	*SS*	*df*	*MS*	F_{stat}	*p-value*	F_{crit}	F_{stat}/F_{crit}
Between Groups	34606	2	17303	0.1610	0.8530	3.8056	0.042
Within Groups	1397329	13	107487				
Total	1431935	15					

Table 28. ANOVA results for the load at CMOD = 3.0 mm for the 150×150 mm² specimens (Mix 1, 40 kg of 35 mm long fibres).

Source of Variation	*SS*	*df*	*MS*	F_{stat}	*p-value*	F_{crit}	F_{stat}/F_{crit}
Between Groups	15423	2	7712	0.0796	0.9239	3.8056	0.021
Within Groups	1258742	13	96826				
Total	1274165	15					

Table 29. ANOVA results for the load at CMOD = 4.0 mm for the 150×150 mm² specimens (Mix 1, 40 kg of 35 mm long fibres).

Source of Variation	*SS*	*df*	*MS*	F_{stat}	*p-value*	F_{crit}	F_{stat}/F_{crit}
Between Groups	43758	2	21879	0.2221	0.8038	3.8056	0.058
Within Groups	1280882	13	98529				
Total	1324640	15					

Table 30. ANOVA results for the dissipated energy for the 150×150 mm² specimens (Mix 1, 40 kg of 35 mm long fibres).

Source of Variation	*SS*	*df*	*MS*	F_{stat}	*p-value*	F_{crit}	F_{stat}/F_{crit}
Between Groups	9561	2	4780	0.1654	0.8494	3.8056	0.043
Within Groups	375827	13	28910				
Total	385388	15					

Table 31. ANOVA results for the maximum load for the 200×200 mm^2 specimens (Mix 2, 40 kg of 60 mm long fibres).

Source of Variation	*SS*	*df*	*MS*	F_{stat}	*p-value*	F_{crit}	F_{stat}/F_{crit}
Between Groups	254253	2	127126	2.2513	0.1447	3.8056	0.592
Within Groups	734070	13	56467				
Total	988323	15					

Table 32. ANOVA results for the load at CMOD = 1.0 mm for the 200×200 mm^2 specimens (Mix 2, 40 kg of 60 mm long fibres).

Source of Variation	*SS*	*df*	*MS*	F_{stat}	*p-value*	F_{crit}	F_{stat}/F_{crit}
Between Groups	2133859	2	1066930	1.3092	0.2992	3.6823	0.356
Within Groups	12224511	15	814967				
Total	14358370	17					

Table 33. ANOVA results for the load at CMOD = 2.0 mm for the 200×200 mm^2 specimens (Mix 2, 40 kg of 60 mm long fibres).

Source of Variation	*SS*	*df*	*MS*	F_{stat}	*p-value*	F_{crit}	F_{stat}/F_{crit}
Between Groups	2116451	2	1058225	1.3258	0.2950	3.6823	0.360
Within Groups	11972739	15	798183				
Total	14089190	17					

Table 34. ANOVA results for the load at CMOD = 3.0 mm for the 200×200 mm^2 specimens (Mix 2, 40 kg of 60 mm long fibres).

Source of Variation	*SS*	*df*	*MS*	F_{stat}	*p-value*	F_{crit}	F_{stat}/F_{crit}
Between Groups	1847508	2	923754	1.1054	0.3566	3.6823	0.300
Within Groups	12534944	15	835663				
Total	14382452	17					

Table 35. ANOVA results for the load at CMOD = 4.0 mm for the 200×200 mm^2 specimens (Mix 2, 40 kg of 60 mm long fibres).

Source of Variation	*SS*	*df*	*MS*	F_{stat}	*p-value*	F_{crit}	F_{stat}/F_{crit}
Between Groups	1568620	2	784310	0.9818	0.3974	3.6823	0.267
Within Groups	11982165	15	798811				
Total	13550785	17					

Table 36. ANOVA results for the dissipated energy for the 200×200 mm^2 specimens (Mix 2, 40 kg of 60 mm long fibres).

Source of Variation	*SS*	*df*	*MS*	F_{stat}	*p-value*	F_{crit}	F_{stat}/F_{crit}
Between Groups	266006	2	133003	1.1083	0.3557	3.6823	0.301
Within Groups	1800054	15	120004				
Total	2066060	17					

Appendix B – Drawings of equipment

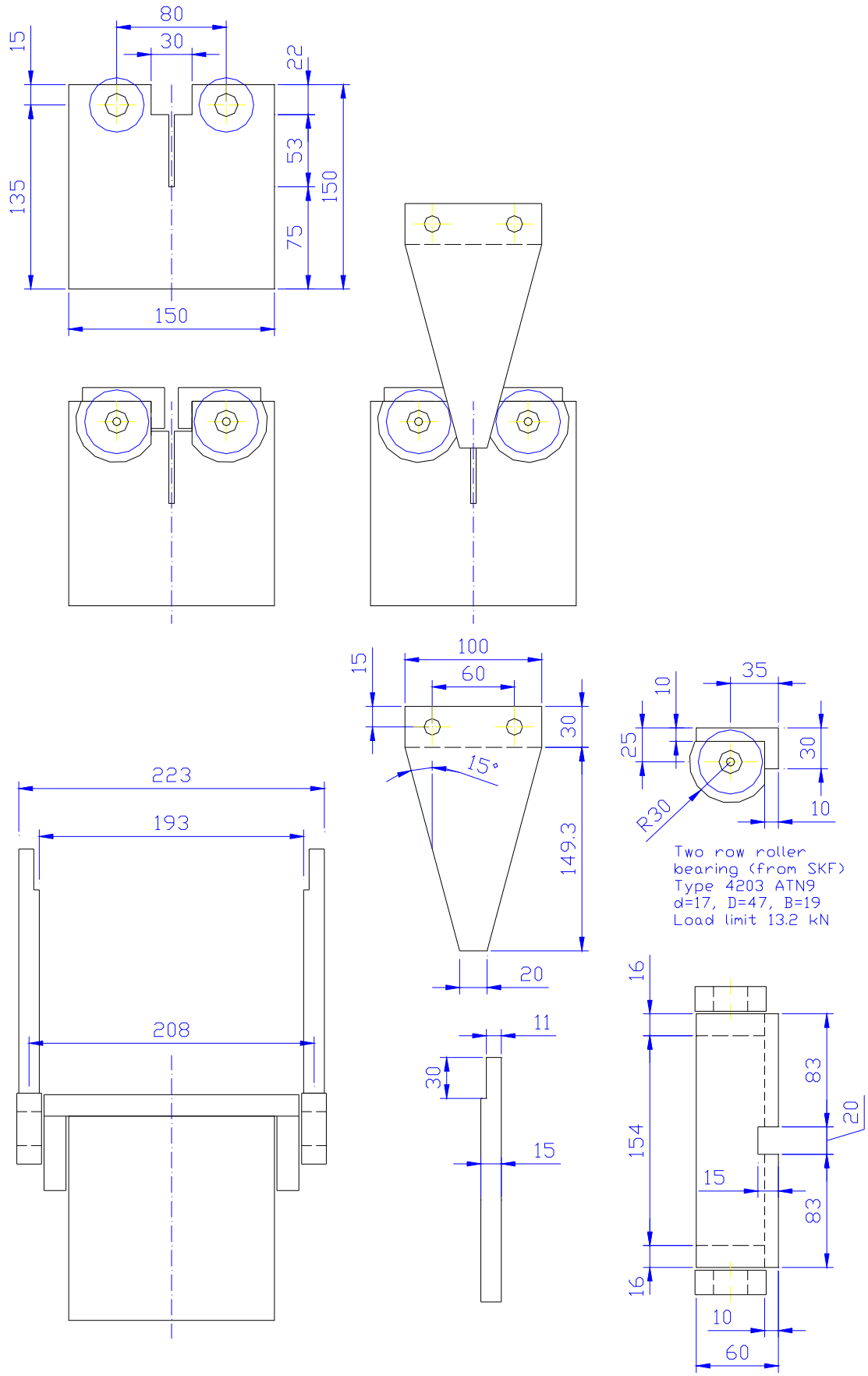

Appendix C – NORDTEST Method proposal

WEDGE SPLITTING TEST METHOD (WST):
FRACTURE TESTING OF FIBRE-REINFORCED CONCRETE (MODE I)

Key words: Fibre-reinforced concrete, fracture testing

1. SCOPE AND FIELD OF APPLICATION

This method specifies a procedure for determining/characterizing the mode I tensile fracture behaviour of fibre-reinforced concrete by means of the Wedge Splitting Test (WST) method on notched specimens.

2. REFERENCES

NT BUILD 201 *Concrete: Making and curing moulded test specimens for strength tests.*

3. SYMBOLS

A_{lig}	Ligament area
CMOD	Crack mouth opening displacement
CTOD	Crack tip opening displacement
D_{max}	Maximum size of the aggregates
F_v	Vertical force
F_{sp}	Splitting force
G_{fCMOD}	Energy dissipated during fracture to a prescribed *CMOD*
L_{fmax}	Maximum length of the fibres
N_F	Total number of fibres crossing the fracture plane
V_F	Volume fraction of fibres
W_F	Work of fracture
b	Width of the specimen/ligament
d_x	The horizontal distance between the loading points
d_y	The vertical distance from the bottom of the specimen to the point where the splitting load is applied
f_{tR}	Residual tensile stress
h_c	Depth of the ligament under the notch
m	Total weight of the specimen
w	Crack opening
x	Height of the compressive zone
α	Wedge angel = 15°

4. SAMPLING

The test is performed on moulded test specimens. The standard testing age is 28 days, but the method can also be used at other ages. Moreover, the test method can also be used for core-drilled samples.

The size of the specimen depends on the purpose of the test and shall, if relevant, be sufficient for the result to be treated statistically and representative. The dimensions of the specimen (height, width, and thickness) should preferably be four times the maximum fibre length (at a minimum, three and a half times).

5. TESTING

5.1 Principle

In Figure 1and Figure 2 the specimen geometry and loading procedure are clarified. The specimen is equipped with a groove (to be able to apply the splitting load) and a starter notch (to ensure the crack propagation). Two steel platens with roller bearings are placed partly on top of the specimen partly into the groove, and through a wedging device the splitting force, F_{sp}, is applied. During a test, the load in the vertical direction, F_v, and the crack mouth opening displacement (*CMOD*) are monitored.

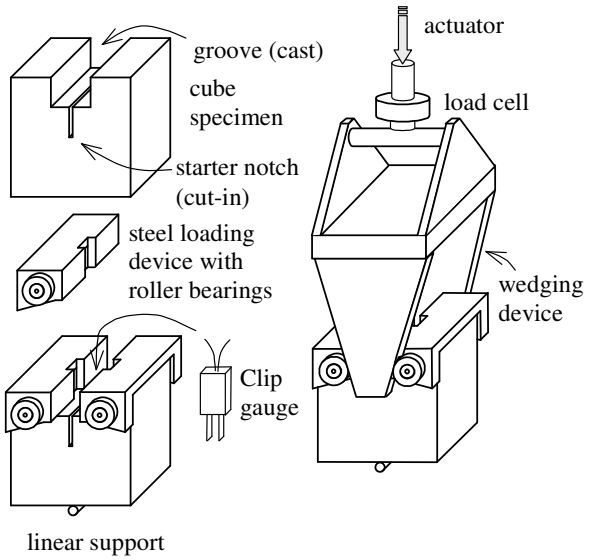

Figure 1. Schematic view of the equipment and test setup.

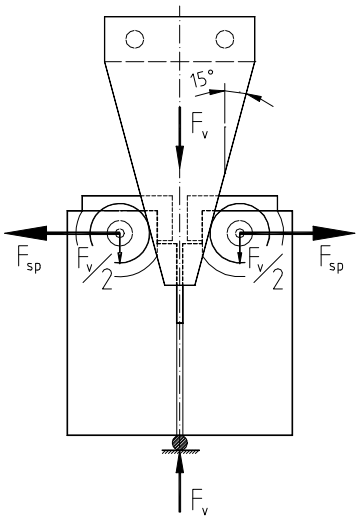

Figure 2. Principle of applying the splitting load.

5.2 Test specimen geometry

For standard testing on cast specimens, the specimen geometry is based on standard cube specimens provided with a cast groove and a sawn starter notch.

The depth of the starter notch shall be equal to half the height of the specimen depth (cut to a precision of ±1 mm). The width of the notch shall not be greater than 5 mm.

The dimensions of the specimen shall not vary more than 2 mm on all sides. Additionally, the differences in overall dimensions on opposite sides of the specimen shall not be greater than 2 mm.

The size of the specimen depends on the maximum fibre length (L_{fmax}) – or maximum size of the aggregate (D_{max}) – it is recommended that the dimension of the specimen (height, width, and thickness) should be at least three and a half (3.5) times larger than the maximum fibre length.

Furthermore, to minimize the influence of wall effects at the formwork surfaces, a guide notch is to be sawed. Moreover, the guide notch is also beneficial as it prevents horizontal cracks from occurring, which may be a problem for high fibre content. The depth of the guide notch is 25 ±1 mm. See Figure 3 for example of specimen geometries.

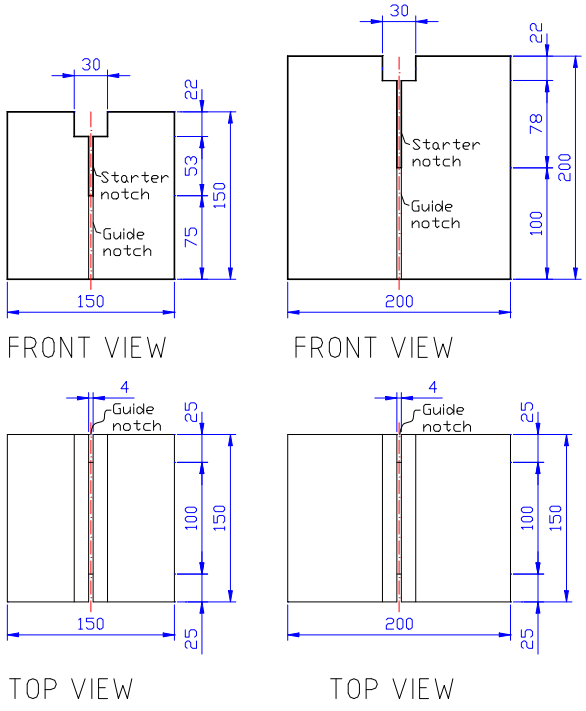

Figure 3. Example of specimen geometries (150×150×150 mm^3 and 200×200×150 mm^3).

5.3 Test specimen preparation

The specimens are to be produced according to the principles given in NT BUILD 201.

After casting and before de-moulding, the specimens are kept in the moulds at +20 ±2

°C and covered with a plastic sheet to prevent evaporation. After de-moulding, not earlier than 16 hours and not later than 48 hours after casting, the specimens are constantly kept in lime-saturated water (+20 ±2 °C) until less than 60 minutes before testing.

The notch shall be sawn under wet conditions not earlier than 3 days after casting and not later than 1 day before testing.

5.4 Equipment

Equipment to support and load the specimen according to Figure 1. is required. The wedge splitting equipment consists of: two steel platen-loading devices (with roller bearings), a linear support, and a wedging device.

The testing system consists of: frame, actuator, load cell, clip gauge (or other measuring device), controller and data acquisition equipment as a minimum. Whereas it is preferable to have a closed-loop controlled machine, this is not required.

The load shall be measured with an accuracy of ±1% of the maximum load value in the test. The displacement-measuring device, measuring the CMOD, shall have an accuracy better than ±0.01 mm.

5.5 Testing environment

The specimens may be removed from the water 60 minutes prior to starting the test.

5.6 Test procedure

Immediately before the test the weight of the specimen is measured with an accuracy of ±10g.

After weighing, the specimen is placed on the support, according to Figure 1., the wedge is lowered and the specimen is pre-loaded to a level of 50 to 100 N. Thereafter the test can begin and the testing machine should be operated so that, in the beginning of the test, the measured CMOD increases at a constant rate of 25 to 50 μm/min for CMOD from 0 to 0.2 mm. For CMOD between 0.2 and 2 mm a constant rate of 0.25 mm/min should be applied. When the CMOD is larger than 2 mm, the rate of loading may be increased to 0.5 mm/min. The changes in the loading rate should be made progressively in such a way that it does not influence the test result – i.e. the changes should not be to abrupt as it may result in an increased load resistance.

The load-CMOD diagram is determined by continuously measuring and logging corresponding values of the vertical load, F_v, and the CMOD. During the first two minutes, data shall be logged with a frequency not less than 5 Hz; thereafter, up to the end of the test, the frequency shall no be less than 1 Hz.

For the test to be valid it is required that the load-CMOD response is stable.

After the test, the area of the fractured ligament is to be measured. The following should be measured with an accuracy of ±0.1 mm: the depth, h_c, and the width, b, of the ligament under the notch.

5.7 Evaluation of the test

The splitting force, F_{sp}, is calculated as:

$$F_{sp} = \frac{F_v}{2\tan(\alpha)} \cdot \frac{(1 - \mu \cdot \tan(\alpha))}{1 + \mu \cdot \cot(\alpha)}$$

where α is the angel between the wedge and the vertical load line and μ is the coefficient of friction between the wedge and the rollers that are used to guide the wedge. As the influence of the friction is small, the relationship may be approximated by:

$$F_{sp} = \frac{F_v}{2\tan(\alpha)}$$

The work of fracture, W_F, is calculated as the area under the splitting load-*CMOD* curve (F_{sp}-*CMOD*). At a specific *CMOD* the energy dissipated during fracture, W_{fCMOD}, is normalised with respect to the total ligament area, A_{lig}, at complete fracture. This intermediate, specific fracture energy is denoted G_{fCMOD} [Nm/m^2], and may be determined directly from the test result by performing the calculation:

$$G_{fCMOD} = \frac{W_{fCMOD}}{A_{lig}}$$

where, W_{fCMOD} is the area under the splitting load-*CMOD* curve and A_{lig} is the area of the ligament (all of the expected total cracked area).

In the WST-method, no measurements are made of the real crack opening – this is often due to measurement technique or due to specific test conditions. As can be seen in Figure 4, while the *CMOD* is measured at some distance from the tip of the notch the *CTOD* is the crack opening at the tip of the notch. The crack tip opening displacement (*CTOD*), however, represents a 'true' crack opening and, thus, is an important parameter when evaluating the fracture properties.

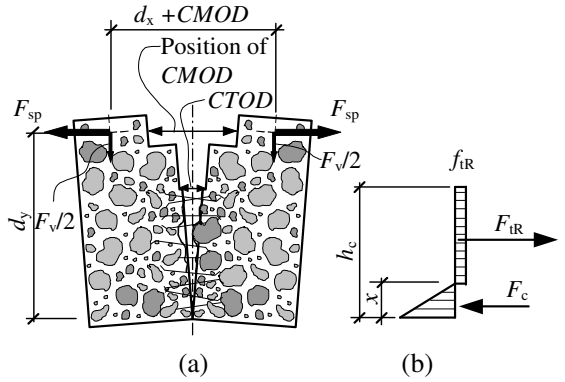

Figure 4. (a) Schematic view of a cracked specimen and the definition of CMOD and CTOD. (b) Simplified stress distribution based on the assumption of a constant residual tensile stress f_{tR} (*x* denotes the height of the compressive zone).

For WST-specimens with the dimensions 150×150 mm^2, the following expression (based on five mixes with the fibre content varying between 0.5% and 1.0 %) has been evaluated for the relationship between the *CMOD* and the *CTOD*:

$$CTOD = 0.551 \cdot CMOD - 0.0084 \text{ [mm]}$$

For WST-specimens with the dimensions 200×200 mm^2, the following expressions have been evaluated for the relationship between the *CMOD* and the *CTOD*:

$$CTOD = 0.533 \cdot CMOD - 0.0110 \text{ [mm]}$$

A simplified approach to determine a residual tensile stress is to use the given relationships between *CMOD* and *CTOD* to calculate an crack opening *w*. With a assumption of the height of the compressive zone, it is then possible to determine the residual tensile stress, f_{tR}, at a specific *CMOD* and calculate the corresponding crack opening, *w*. If a constant residual tensile stress f_{tR}, is assumed and that the height of the compressive zone is given by:

$$x \approx \frac{h^*}{10}$$

then the residual tensile stress, f_{tR} can be calculated by solving the equilibrium equation of forces and the equilibrium equation of moment with respect to the position of the neutral axis (see Figure 4):

$$F_{tR} - F_c - F_{sp} = 0$$

$$F_{tR} \cdot \left(\frac{h_c - x}{2}\right) + F_c \cdot \left(\frac{2}{3}x\right) - F_{sp}\left(d_y - x - \frac{(CMOD/2)^2}{d_y - x}\right) - \frac{F_v}{2}\left(\frac{d_x + CMOD}{2}\right) = 0$$

$$\Rightarrow f_{tR} = \frac{F_{tR}}{(h_c - x) \cdot b}$$

where: d_x is the horizontal distance between the loading points (for the undeformed specimen); d_y is the vertical distance from the bottom of the specimen to the point where the splitting load is applied; h_c is the depth of the ligament; and *b* is the width of the ligament.

5.8 Uncertainty

The scatter in the test result is dependent on the fibre distribution in a specimen, the variation in fibre content between specimens, the amount of fibres, the fibre length. The coefficient of variance can expected to vary between 5 percent and 40 percent (for the applied splitting load at a given *CMOD*). For this reason, it is recommended that six specimens should be tested.

6. TEST REPORT

The test report shall include the following information.

I. General information

a) Address of the testing laboratory and name of the person responsible.

b) Identification number of the test report.

c) Name and address of the organization, or person, who ordered the test.

d) Purpose of the test.

e) Date of the test.

II. Description of the material tested

f) Description of the method of producing the specimens.

g) Description of the tested concrete.

h) Age of the tested specimens.

III. Test method

i) Individual geometry of the specimens.

j) Device and set-up for loading, support, measurements, and recording.

k) Rate of *CMOD* or rate of vertical displacement.

l) Climate in test laboratory.

m) Any deviation from this standard.

IV. Test results

n) Test result in the form of splitting load-*CMOD* curves.

o) The energy dissipated during fracture.

p) Total number of fibres, N_f, crossing the fracture plane, and a note on the fibre distribution.

Depending on the purpose of the test and the number of specimens, it may be also relevant to include, e.g. the load-CMOD curve of each specimen and statistical evaluation of the test.

7. LITERATURE

Brühwiler, E. and Wittmann, F.H. (1990): 'The wedge splitting test, a new method of performing stable fracture mechanics test' *Eng. Fracture Mech.* 35(1/2/3), 117-125.

de Place Hansen, E.J., Hansen, E.A., Hassanzadeh, M., and Stang, H. (1998): Determination of the Fracture Energy of Concrete: A comparison of the Three-Point Bend Test on Notched Beam and the Wedge-Splitting Test. NORDTEST Project No 1327-97. SP Swedish National Testing and Research Institute, Building Technology, SP Report 1998:09, Borås, Sweden. p. 87.

Elser M., Tschegg E.K., Finger N., and Stanzl-Tschegg S.E. (1996): 'Fracture Behaviour of Polypropylene-Fibre reinforced Concrete: an experimental investigation', *Comp. Science and Technology*, 56(1996), pp. 933-945.

Linsbauer, H.N. and Tschegg, E.K. (1986) 'Fracture energy determination of concrete with cube shaped specimens', *Zement und Beton*, 31, pp 38-40.

Löfgren I, Stang H, and Olesen JF (2004): *'Wedge splitting test – a test to determine fracture properties of FRC'* BEFIB 2004 - Sixth RILEM symposium on fibre reinforced concrete (FRC): Varenna, Italy, 20th-22nd September 2004.

RILEM Report 5 (1991): *Fracture Mechanics Test Methods for Concrete*. Edited by S.P. Shah and A. Carpinteri. Chapman and Hall, London, 1991.